MICROCOPY RESOLUTION TEST CHART

NATIONAL BUREAU OF STANDARDS-1963-A

AD A064067

LEVEL

13 67 p.

11 Dec 78

6 DAMAGE STUDIES OF ION-IMPLANTED GaAs
USING CONDUCTIVITY PROFILES.

THESIS

14 AFIT/GE/EE/78D-43   10 Russell M./Solt
Capt   USAF

9 Master's thesis,

DDC
RECEIVED
FEB 2 1979
A

79 01 30 105
012 225

DAMAGE STUDIES OF ION-IMPLANTED GaAs

USING CONDUCTIVITY PROFILES

THESIS

Presented to the Faculty of the School of Engineering

of the Air Force Institute of Technology

Air Training Command

in Partial Fulfillment of the

Requirements for the Degree of

Master of Science

by

Russell M. Solt, B.S.

Capt   USAF

Graduate Electrical Engineering

December 1978

Contents

List of Figures

List of Tables

Abstract

  The understanding of damage produced during ion-im
plantation is an important first step towards predicting
the semiconducting behavior of GaAs samples. A new tech-
nique for measuring damage has been developed by the Air
Force Avionics Laboratory. This method involves the meas-
urement of a differential electrical conductivity profile.

  Samples of GaAs doped with S^+, Te^+ and Ar^+ ions were
prepared for the purpose of profiling them with this
technique. Prior to measurement, theoretical values of
critical dose and theoretical damage profiles were calcu-
lated using damage-range theory.

  Values of sheet conductivity were measured with an
electrical measurement system. Twenty-four samples of
varying dose, flux and implant type were used. Each sample
was profiled by measuring sheet conductivity at successively
deeper levels into the sample. A soulution of H_2SO_4 :
H_2O_2 : H_2O was used to etch the samples to arrive at these
deeper levels. The thickness etched away was determined by
the use of a Sloan Dektak Surface Profile Measuring System.

  The values of sheet conductivity measured along with
the thickness etched away were used to create bulk conduc-
tivity profiles for all of the samples. The normalized
profiles are used to show damage versus depth. The measured
values of critical dose and damage agree within an order of
magnitude of those predicted by theory.

Future efforts might include automating the measurement system, refining the theory to account for any deviations observed and to vary certain controllable parameters of the ion-implantation process and observe what changes in damage they produce.

DAMAGE STUDIES OF ION-IMPLANTED GaAs
USING CONDUCTIVITY PROFILES

I   Introduction

Ion implantation is being widely used as a means of
introducing dopant impurities into GaAs. One fundamental
problem associated with ion-implantation is that of lattice
damage. Lattice damage, which is an inevitable by-product,
reduces, if not destroys, the usefulness of any device fab-
ricated by the ion-implantation technique. For this reason,
the implanted samples require special annealing processes
in which the samples are heat-treated at temperatures of
$800\text{-}900^{\circ}C$ to remove radiation damage produced during im-
plantation and to cause a substantial fraction of the im-
planted ions to become electrically active. An understanding
of damage produced during implantation is an essential first
step in predicting the semiconducting behavior of samples
after annealing.

In the past, several techniques have been developed and
used for measuring damage. Included in these techniques are
electroreflectance, photoluminescense and Rutherford back-
scattering. These methods involve costly equipment and
exhaustive techniques and yield questionable results when
compared with damage theory.

Recently, the Air Force Avionics Laboratory proposed a new approach to the damage problem which is now being developed. This method involves the measurement of a differential electrical conductivity profile (DECP). The surface conductivity of a sample can be measured using a Vander Pauw electrical measurement system. By successive etchings and measurements of each new surface, a conductivity profile can be obtained. It has been shown that when normalized, this profile agrees strongly with theoretical damage profile predictions for the specific cases of GaAs implanted with C^+, Mg^+ and Cd^+ ions. (Ref 1:3)

This thesis describes the result of efforts to expand the data base needed to evaluate the damage theory. Samples of GaAs implanted with S^+, Te^+ and Ar^+ ions were profiled with the objective of showing that the relationship between experiment and theory holds for any implanted substance whether it produces p-type, (C^+, Mg^+, Cd^+), n-type, (S^+, Te^+), or neutral, (Ar^+), GaAs.

This thesis first presents a general overview of ion-implantation, damage range theory and differential electrical conductivity profiles. Following this, the experimental setup and procedures are described in detail. The process by which raw data is converted into damage profiles is presented next along with the actual profiles obtained. These are then compared with the theoretical profiles and comments made. Finally, some suggestions for further research and recommendations are given.

II   Theory/Background

There are basically three areas which must be examined
to develop an understanding of damage profiles. First the ion-
implantation process is discussed as an aid to understanding
the mechanism of damage. Second, the damage-range theory is
presented for use in comparing with the experimental data.
Finally, a brief discussion of the relationship between dam-
age and the measurement of electrical conductivity is pre-
sented as an introduction to the remainder of this report.

The Process of Ion-Implantation

Ion-implantation is an inherently complex method of pro-
ducing semiconductor materials with a precisely controlled
fraction of electrically-active impurities. Implantation
technology is the only processing technique which allows
unambiguous introduction of a single dopant species into the
host material. The final atomic concentration and uniformity
of the dopant impurities can also be controlled in a more
efficient manner than is possible using other techniques.
(Ref 2:2) Ion-implantation can also be used in conjunction
with other fabrication techniques to produce device structures
that no single process can produce alone. (Ref 3:295)

The doping of semiconductor materials by ion-implantation
is accomplished by directing 10-150 keV ion beams of momen-
tum-analyzed ions onto the target material. These ions,
typically produced in a small accelerator, are momentum-
analyzed to provide an atomically pure dopant source. (Ref 2:2)

3

When a substrate is bombarded by a beam of these energetic ions, it will not only loose some of its own ions by sputtering but it will also retain some of the incident ions. The incident ions that are retained are said to be implanted. (Ref 3:295)

The disadvantage of ion-implantation is the crystal damage produced at the surface of the semiconductor as the ions collide with the lattice atoms. The implantation damage can be minimized by annealing the crystal at high temperatures, but annealing also causes the impurity profile to diffuse into the crystal thus changing the desired dopant profile. Knowing the lowest effective annealing temperature and time is important to minimize this diffusion. (Ref 4:2) For this reason it is important to be able to predict damages.

The Damage-Range Theory

As energetic ions penetrate the target, they lose energy primarily through two independent types of collisions before coming to rest. These collisions are called elastic and in-elastic. Inelastic (electronic) collisions leave the electrons of the host atom in an excited state but the center-of-mass motion of the target atom is unperturbed. Only the elastic (nuclear) collision process creates lattice disorder around the ion track and is responsible for radiation-damage effects. (Ref 1:3) Furthermore, if the target is crystalline, the target atoms will be bound to their lattice positions with a certain energy, so that collisions of the projectile with the atoms of the target will only produce damage when the

4

energy transferred to a target atom exceeds its displacement threshold energy, E_d.

Collisions in which the energy transferred to a target atom, say E', is greater than E_d will displace that atom from its lattice site, and thus produce damage within the crystal. The displaced target atom may then be treated as a secondary projectile of energy $(E' - E_d)$, and it too will be brought to rest through a series of nuclear and electronic stopping events. In the course of its trajectory, the secondary projectile may have sufficiently energetic interactions with other target atoms to produce further displacements and a second generation of recoiling target atoms. The production of damage is therefore a cascade process in which the incident projectile is simply the primary damage-producing particle. The envelope of all these displacements is referred to qualitatively as a "damage cluster", and will have a size and character that depends on a large number of factors, including especially the mass of the incident ion and its energy, the mass of a target atom and the temperature of the target. (Ref 5:1063)

The "critical dose", $\emptyset_{crit}$ (i.e. the point at which the sample becomes totally amorphous), can be estimated by a very simple calculation. By definition, the critical dose for a sample of unit volume occurs when all atoms, N in the sample are displaced by the incoming ions. If the atoms are held in the lattice by an energy, E_d, then an ion with initial energy E_o could displace a maximum of E_o/E_d atoms. The min-

5

imum critical dose per unit volume is therefore equal to
$N/(E_o/E_d)$. However, since E_o is dissipated by elastic and
inelastic collisions and only the elastic or nuclear colli-
sions cause damage, E_o must be replaced by $(E_o)_n$, the energy
dissipated in nuclear collisions, thus:

$$\phi_{crit} = N/((E_o)_n/E_d) \qquad (1)$$

Approximate values of ϕ_{crit} obtained with this equation are
shown in Table I for GaAs ion-implanted at room temperature
with S^+, Te^+, and Ar^+ ions with $E_o = 120$ keV. Appendix A
contains the actual numerical calculations from which these
values were obtained.

TABLE I

Theoretical Values of ϕ_{crit}

Ion Implanted	ϕ_{crit} (cm^{-2})
S^+	1.653×10^{14}
Te^+	2.425×10^{13}
Ar^+	1.119×10^{14}

Knowledge of the gross damage-estimate is important,
as is the spatial distribution of the damage in the implanted
layer. It is possible to obtain theoretical damage profiles
by evaluating the spatial distribution of that fraction of
the energy which is ultimately transferred from the implanted
ion to the solid by elastic collisions. The relation which
gives the nuclear energy loss per unit length, $(dE/dX)_n$, is:

6

$$\left(\frac{dE}{dX}\right)_n = \int_0^{E_o} P(E|X,E_o) \, S_n(E) \, dE \qquad (2)$$

where $P(E|X,E_o)dE$ is the energy distribution function and denotes the probability that an ion has energy between E and $E+dE$, given that it was injected into a target at $E=E_o$ and has reached a position X along its track. $S_n(E)$ is the average nuclear energy loss rate given by the Thomas-Fermi nuclear stopping power for an ion. Because all ions do not have the same range, however, we must use separate S_n curves for each ion, thus the need for the integral. (Ref 5:1075)

Given a computation of $(dE/dX)_n$, the number of atoms displaced by the "average" ion should become:

$$N_d = E_n/2E_d \qquad (3)$$

where E_n is simply the area under the $(dE/dX)_n$ curve. (Ref 5:1080)

If damage is defined as displaced atoms then a "damage profile" can be created by differentiating N_d over X. The damage profile is therefore given by:

$$\text{Damage } (cm^{-3}) = \frac{1}{2E_d}\int_0^{E_o} P(E|X,E_o) \, S_n(E) \, dE \qquad (4)$$

When the above equation is solved for a specific case, a theoretical damage profile is obtained. Figures 1 and 2 show graphically this theoretical distribution of damages for GaAs doped with S^+ and Te^+ ions. (Ref 6) Theoretical curves for

7

Ar^+ are not given, however, they closely approximate those for S^+. This is due to the close proximity of argon and sulfur on the periodic table. Figures 1 and 2 also cover only the peak regions of the curves. Beyond the peaks, the damage "tail" behaves as an exponential decay and on a semi-log scale graphs into a straight line.

Conductivity as a Measure of Damage

Impurity-conduction in semiconductors can be defined as a phenomenon in which an electron moves directly (by tunnelling) from one impurity atom or point defect to another. (Ref 7:1) This defect conduction is often referred to as hopping conduction in crystalline semiconductors and low-temperature conduction in amorphous materials. The current produced by these mechanisms depends on the mobility of electrons with energies at or near the Fermi energy. (Ref 7:39) Furthermore, there is evidence that structural defects play a more effective role than do impurities in controlling the conductivity of amorphous semiconductors. (Ref 7:198)

When a sample of GaAs undergoes ion-implantation, it sustains a large amount of damage. This damage takes the form of many point defects. These defects not only increase the defect conduction of the sample, but also bring the structure of the substrate closer to being amorphous. It follows, therefore, that the conductivity of the semi-insulating GaAs substrate increases with implantation dose. Increased damage produces increased

8

conductivity until the sample is totally damaged to the
point where conductivity becomes saturated. (Ref 1:5)
A conductivity profile of ion-implanted GaAs gives definite
values of conductivity as a function of sample depth which
can be correlated specifically with damage-density profiles
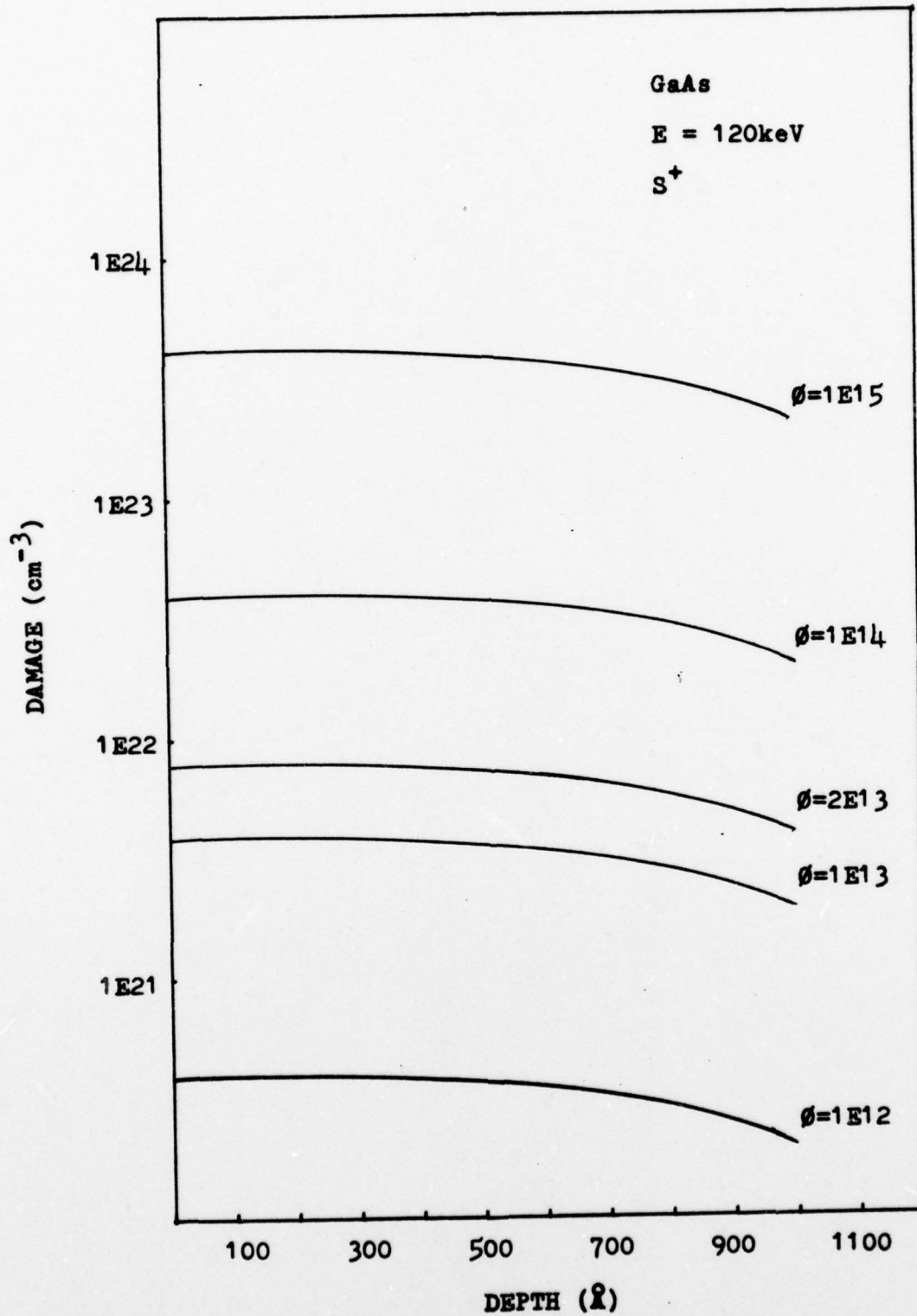of the implanted samples. (Ref 8:14)

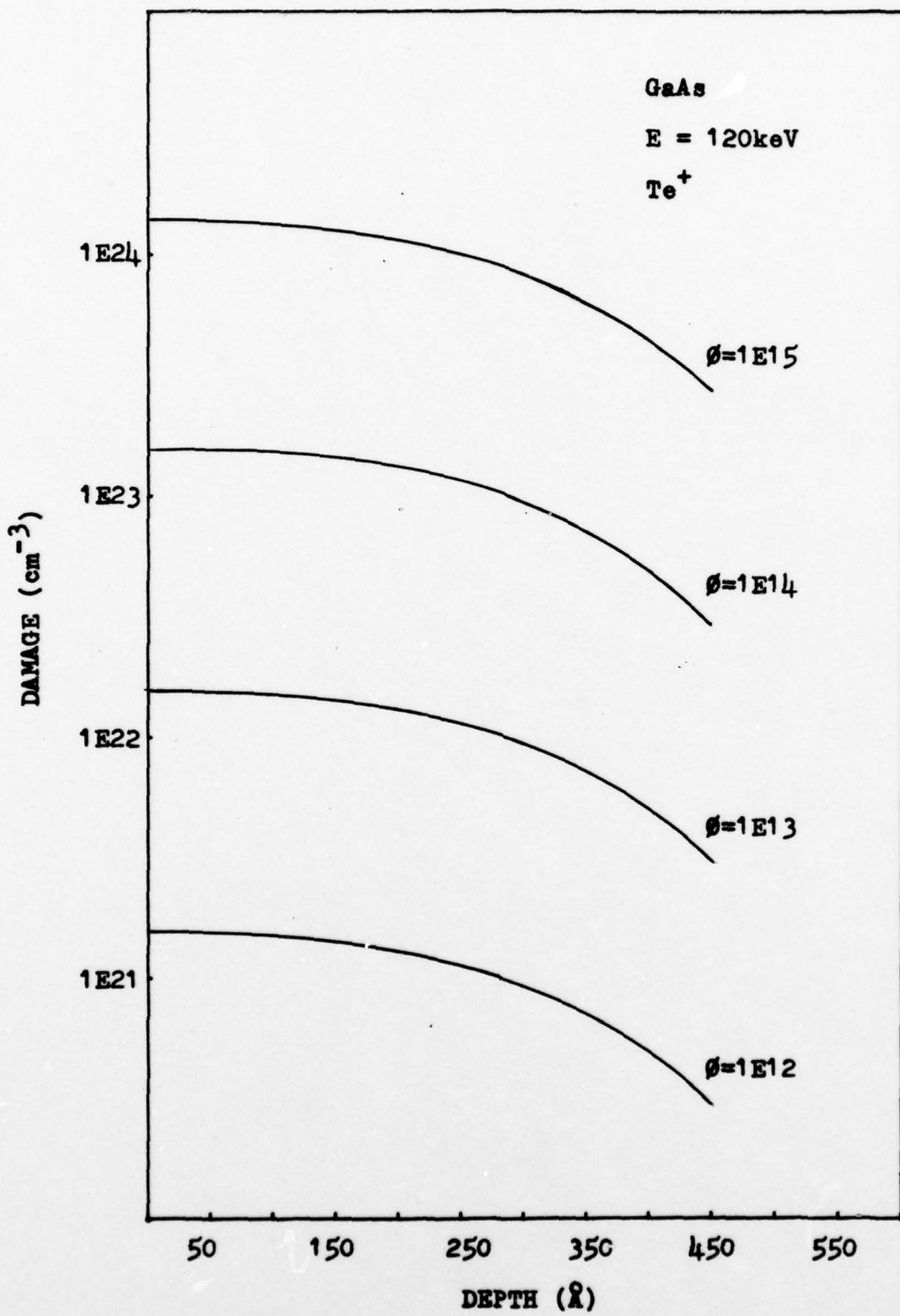Figure 1   Theoretical Damage Profiles for S⁺

Figure 2   Theoretical Damage Profiles for Te$^+$

11

III   Experimental Apparatus

The electrical measurement system used for this experiment
consisted of a Keithly 225 constant current source, a Keithly
616 digital electrometer used as an ammeter for monitoring
current, a Keithly 160 digital voltmeter and two Keithly 610C
electrometers used as unity-gain amplifiers. Figure 3 shows
this system as well as the configuration of the connections
to the samples. It should be noted that this system makes
use of the guarded unity-gain amplifiers to provide the high
input impedance of approximately 10^{14} ohms which is essential
for measurements of high resistivity samples. (Ref 2:53)

A Sloan Dektak Surface Profile Measuring System was used
for the purpose of measuring the thickness of the layer
etched away from the samples. A Peacock micrometer was used
to measure specimen dimensions.

The substrate material used for the samples was Cr-doped,
semi-insulating, single-crystal GaAs sliced into wafers and
oriented in the $\langle 100 \rangle$ direction. Bulk resistivity, ρ of
the wafers was $10^9 \Omega$-cm. Into these substrates, using a 150
kV ion-accelerator manufactured by Accelerators Inc. (model
#700-101, modified), S^+, Te^+ and Ar^+ ions were implanted at
120 keV to various concentrations at various flux rates.
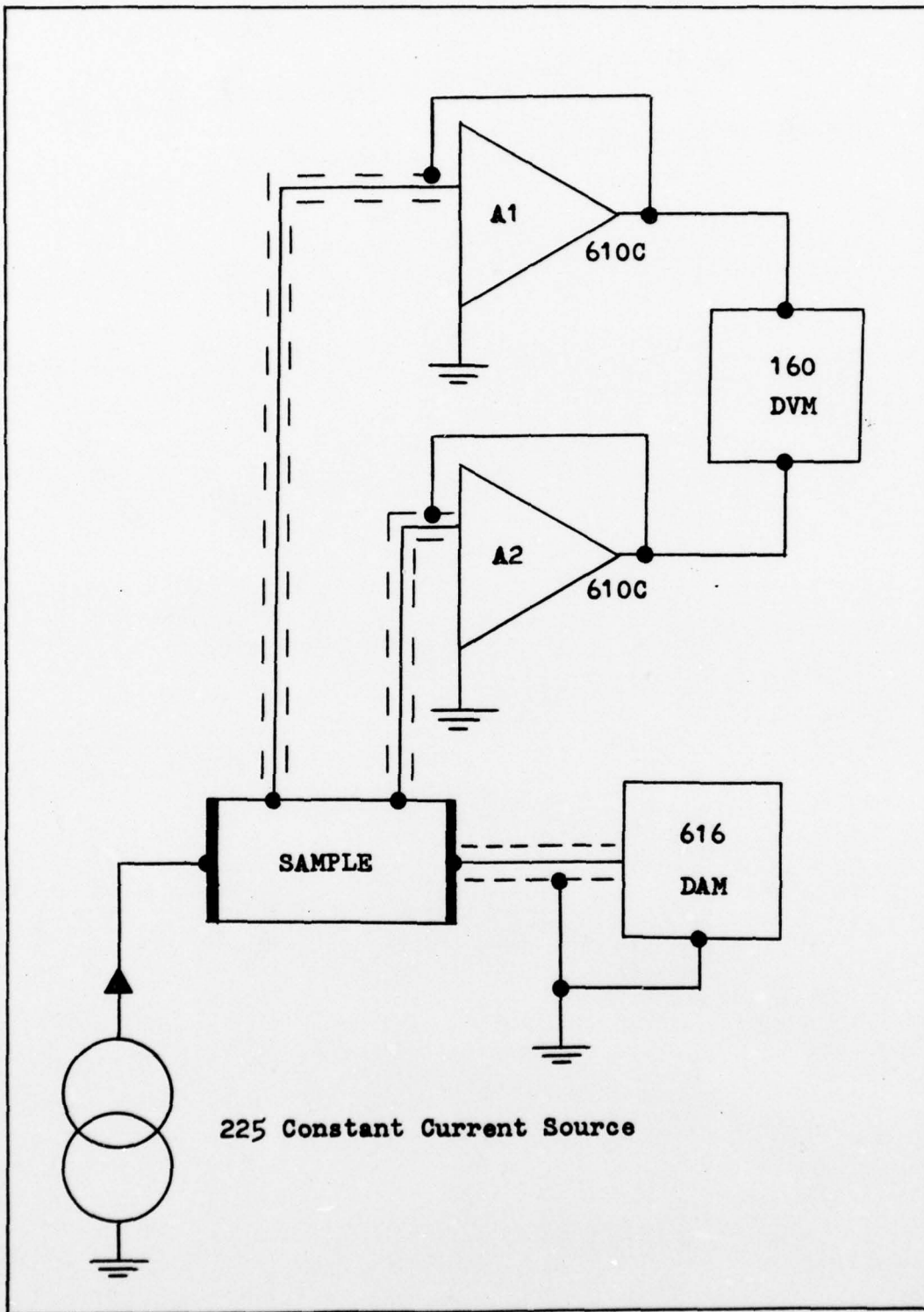Table II summarizes the samples used for this thesis.

Figure 3   Electrical Measurement System

TABLE II

Summary of Samples

Ion	dose, ϕ, (ions/cm^2)	flux (nA/cm^2)	# of samples
S$^+$	1E12	10.45	1
S$^+$	1E13	10.45	2
S$^+$	2E13	127.27	2
S$^+$	1E14	10.45	1
S$^+$	1E14	127.27	2
S$^+$	1E15	127.27	1
Te$^+$	1E12	12.35	2
Te$^+$	1E13	12.35	1
Te$^+$	1E13	123.46	2
Te$^+$	1E14	12.35	2
Te$^+$	1E14	123.46	1
Te$^+$	1E15	123.46	1
Ar$^+$	1E12	16.46	1
Ar$^+$	1E13	164.61	2
Ar$^+$	1E14	164.61	1
Ar$^+$	1E15	164.61	1

IV   Experimental Procedure

The experimental procedure discribed below is one which,
due to the nature of this thesis, was repeated many times,
over a period of several months. As experience was gained
in each task, certain modifications were made to improve the
results obtained or increase the reliability of the measure-
ments. What will be described in the following pages is
the final, refined technique. Where necessary, for clarity,
a brief explanation is given of certain elements of the
procedure. These explanations include observations from
experience and thus summarize the evolution of the experiment.

Mounting the Samples

The samples, as used, were approximately 1 x .5 cm in
size. Four wires were attached to these samples in the
configuration shown in figure 3. Great care was required
in order to assure that strong, ohmic contacts were made.
For a given sample, Indium (In) solder was first applied,
creating two "beads" of solder at points one and two, and two
"lines" of solder at both ends, spanning the width of the
sample. This solder was applied in a minimum of time to
preclude partial annealing of the sample due to heat from
the iron. Also, it was found that better contacts were ob-
tained when the sample was cleaned just prior to applying
the solder. Cleaning the sample involved applying trichloro-
ethylene, acetone, methanol and de-ionized water in succession
to the surface for about thirty seconds each, and finally

15

blow-drying the sample using nitrogen gas. At this point in the procedure, a representative number of samples were placed on a curve tracer to assure ohmic contacts were being created.

The four wires were part of a holder which allowed the samples to be mounted and then plugged into the system by means of a cable and plug assembly. The wires at points three and four were attached to a line of solder to assure even current flow across the entire sample.

Once the wires were attached, the contacts had to be covered with a wax substance. This was done to prevent the contacts from being etched when the sample was profiled. Also, a small wax dot was placed somewhere on the sample so that after the sample had been etched, the thickness etched away could be measured. This dot, it was found, worked best when placed near the center of the sample because the etch rate at the edges was unreliable. An alternative to this procedure was used on several samples. This involved removing a small piece of the sample and mounting it separately on a glass slide. Wax was applied to a portion of this piece and the thickness of the sample etched away was measured from this piece.

Electrical Measurements of the Samples

The sample, mounted on the holder, was plugged in and covered with a black cloth. This was done to eliminate any possible stray photocurrents which might have been present from light falling on the sample.

At this point, current from the constant current source was applied to the sample, first at low levels, and then raised until a voltage of from one to ten volts was displayed on the DVM. The value of current was noted and recorded along with the voltage it produced. To assure the reading was accurate, a check for ohmic-contacts was next performed. The polarity of the current was reversed and the new value of voltage read. When the contacts were ohmic, both values

of voltage were approximately the same except for reversal in sign. The two values of voltage were then averaged together and this average voltage, along with the current were recorded for later use.

When dealing with high resistivity measurements such as those described above, the tendency was for the readings to require a certain amount of time before they settled down to a final value due to stray capacitance. Not waiting long enough created errors. It was found that waiting twenty minutes before taking a reading resulted in satisfactory results.

Etching the Samples

The determination of damage is based on a conductivity profile. The above procedure for measuring voltage and current had to be performed a number of times for each sample at various depths into the implanted layer. In order to accomplish this, successive etchings of the surface were performed between measurements.

The samples were etched in a solution of H_2SO_4 : H_2O_2 :

17

H_2O which was kept at $0^{\circ}C$ by an ice bath and constantly stirred by an electric Stir-Plate. Concentrations varied over the course of these experiments depending on the implant and dose. It was found that great care must be taken when measuring the proportions of H_2SO_4 and H_2O_2 to water in order to obtain a predictable etch rate. Solutions varied from 1:1:30 to 1:1:100 and gave etch rates from approximately 500 to 50 $\mathring{A}$/minute.

From the etch solution the samples were immersed in DI water and then dried using filter paper and nitrogen gas. Extreme care was required during the entire etch/dry process to avoid mishandling the sample and shaking a contact loose. It was possible to only partially loosen a contact causing false changes in conductivity thus invalidating the data.

During the course of profiling a sample, second and third wax dots were sometimes applied to the sample as a way of obtaining more accurate depth information. It was found that the addition of wax to the surface also changed the value of conductivity, giving a false reading. Because of this, when a wax dot was applied, the data point at that depth had to be disregarded.

Measuring the Dimensions of the Samples

With the completion of all conductivity measurements, the wax was removed and the sample cleaned using the same procedure described in the section on mounting the sample. The four wires were removed from the sample and, using a Peacock micrometer, the width of the sample (y) and the
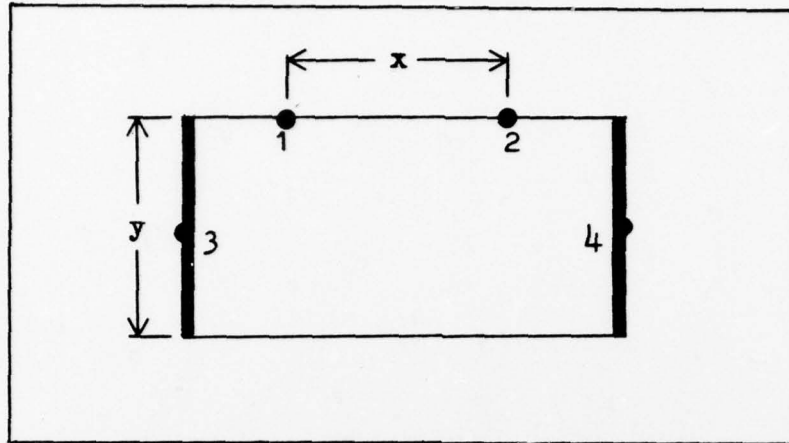
18

Figure 4   Sample Dimensions

distance between contacts one and two (x) were measured
and recorded. Figure 4 shows these distances.

One final measurement was required before the data for
one sample was complete. The etched sample was placed on the
Sloan Dektak Surface Profile Measuring System and a profile
of the sample at the edge(s) of the wax dot(s) was recorded
on a strip chart. From this chart the difference between
the unetched surface which was under the wax dot and the
etched surface could be measured. This value was then divided
by the number of etches performed to obtain an average depth
into the sample per etch. Etch time and strength was main-
tained constant during the profiling of a sample to assure
layers of equal thickness were removed during each etch.
On occasions when the time and/or etch strength was changed
during the profile of a given sample, a wax dot was placed
on the sample to mark where one average thickness ended and
a new one began.

V   Results and Discussion

The raw data obtained from the experiments as described
in the previous chapter had then to be converted, through
a number of steps, into damage profiles. This section
describes how sheet conductivity is calculated. Using
the initial values of sheet conductivity for all samples,
$\emptyset_{crit}$ for each ion is then determined and compared to
those values predicted in Chapter II. Using the values
of sheet conductivity calculated for a given sample, the
derivation of a conductivity profile is discussed. It is
then shown how the conductivity profiles can be normalized
and thus transformed into damage profiles.

The damage profiles obtained from experiment are then
compared to those predicted from theory in Chapter II. On
the basis of these results, observations and conclusions
are presented.

The Sheet Conductivity Measurement

Using the values of current and voltage determined from
experiment and the values of x and y as measured with the
micrometer, the sheet conductivity, σ_s, can be calculated
using the following equation:

$$\sigma_s = \frac{I_c}{V_c} \; \frac{x}{y} \tag{5}$$

A value of sheet conductivity will be available for each
set of voltage and current measurements taken.

As expected, the initial values of σ_s for a given implant type increased with increased dose to a maximum. This reflects the fact that as dose increases, damage increases, until the damage at the surface of the sample is saturated at some $\emptyset_{crit}$. Increasing the dose beyond this point resulted in the value of σ_s actually <u>decreasing</u>. This can be explained by assuming that the additional energy imparted to the surface by the higher dose has the effect of annealling some of the damages already produced thus lowering the value of σ_s. Figures 5 through 7 show graphically the values of σ_s measured for different values of $\emptyset$. It should be noted that these graphs agree strongly with the calculated values of $\emptyset_{crit}$ in Chapter II.

The Conductivity Profile

Sheet conductivity in itself does not provide the information needed to predict damage profiles. Values of bulk conductivity as a function of depth are what is required. Bulk conductivity, or simply conductivity, can be expressed as the derivitive of sheet conductivity:

$$\sigma = \frac{d\sigma_s}{dx} \tag{6}$$

At this point, a simplification will be made by assuming the conductivity at point "1" is equal to:

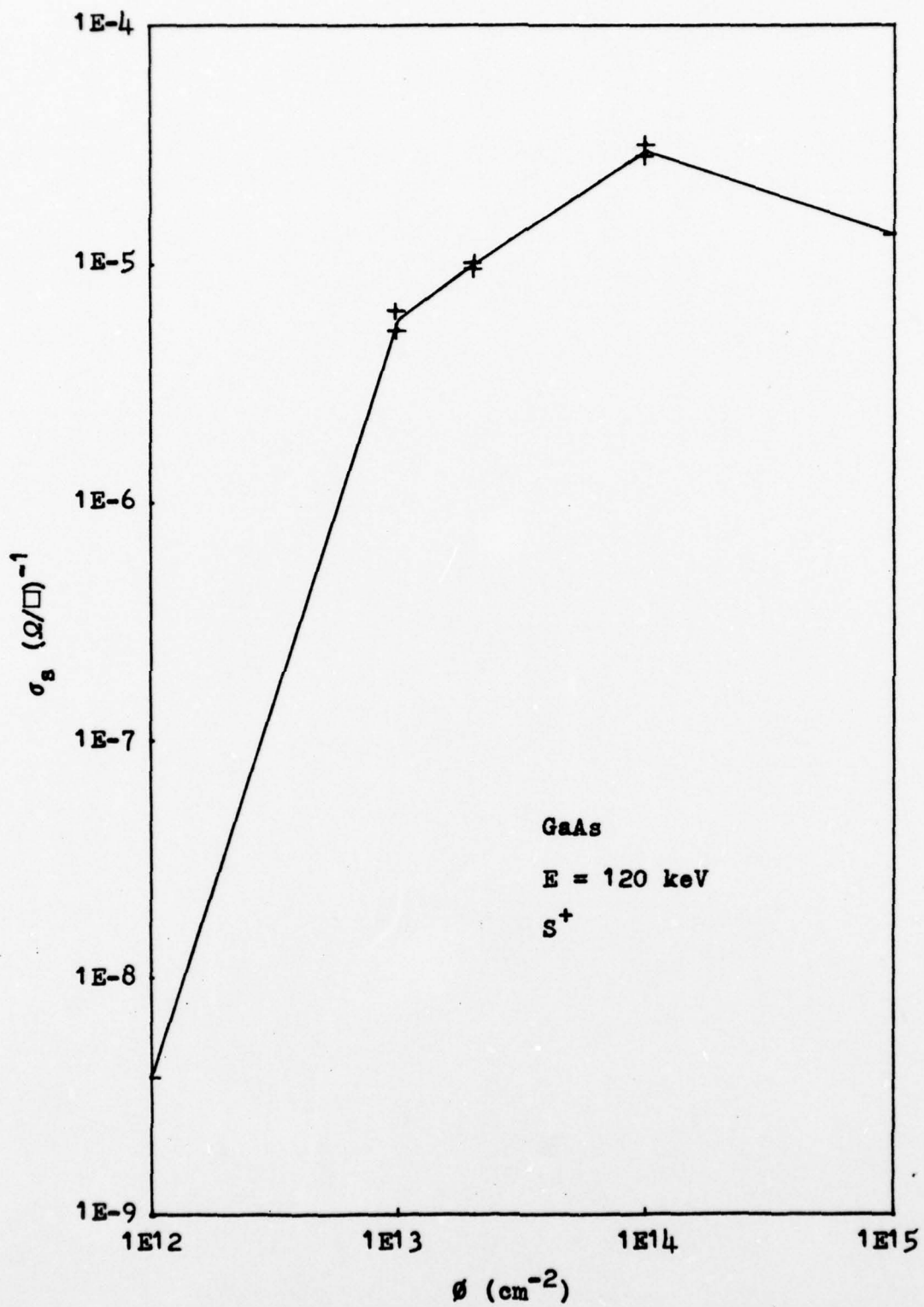$$\sigma_1 = \frac{(\sigma_s)_i - (\sigma_s)_{i+1}}{\Delta x} \tag{7}$$

21

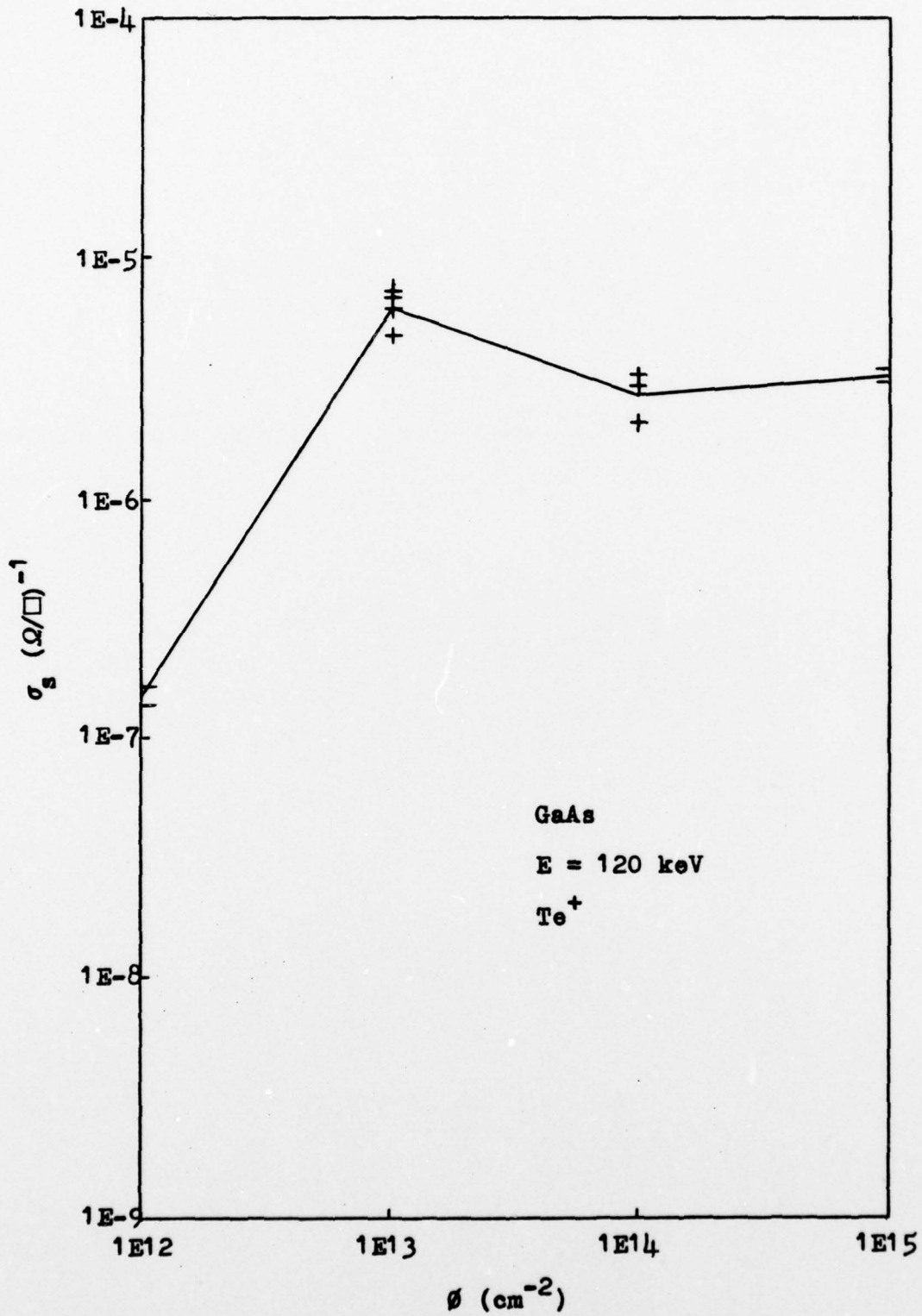Figure 5   Sheet Conductivity versus Dose for S$^+$
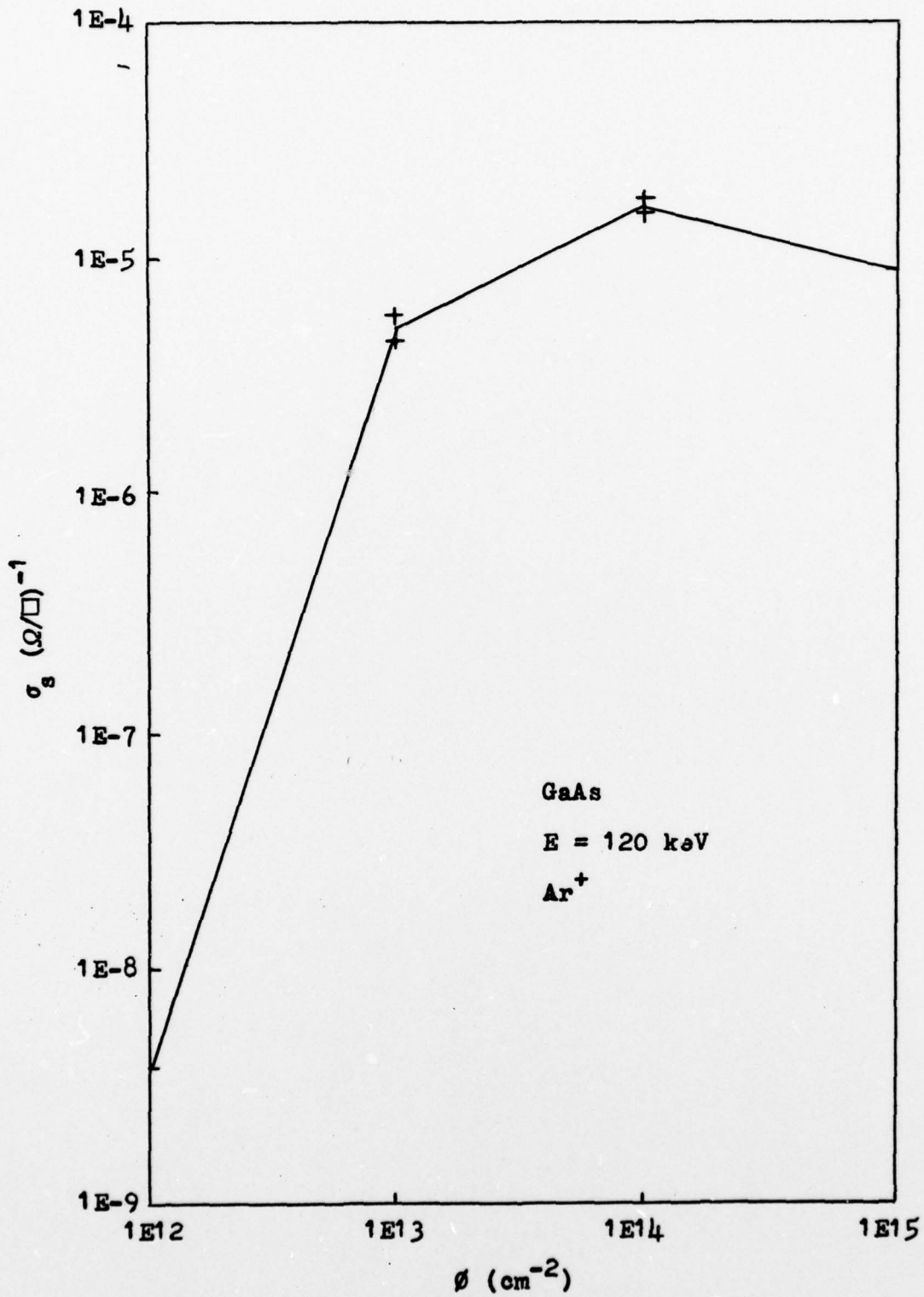
Figure 6   Sheet Conductivity versus Dose for Te$^+$

23

Figure 7   Sheet Conductivity versus Dose for Ar^+

Using equation 5, the values of σ_s calculated for a given sample and the average depth etched as measured on the Dektak, a graph depicting the conductivity profile can be created by plotting the values of σ_i versus the depth at point "i" and then connecting the points with a smooth curve.

Through the course of this research, twenty-three profiles covering sixteen different sample types were measured. These can be found in Appendix B. Table III is a summary of these curves. For each sample type, the approximate value of the peak conductivity is given along with the depth into the sample at which it occurs. Also, the "spread" of the curve is given. Spread is defined as the difference between the peak value of conductivity and the depth at which the conductivity is down 50%.

The Damage Profile

Converting a conductivity profile into a damage profile is basically a matter of normalization. Earlier in this paper it was stated that, above a certain dose, $\emptyset_{crit}$, the damage to the crystal becomes saturated and equates to 100% of the atoms being displaced (i.e. the sample becomes totally amorphus). It follows, therefore, that the maximum value of σ obtained equates to 100% damage. In GaAs there are approximately 4.4×10^{22} atoms/cc. By using the following relationship, values of conductivity can be converted to numbers of atoms displaced:

TABLE III

Summary of Conductivity Profiles

SAMPLE Ion/Dose(ions/cm^2) /Flux(nA/cm^2)	PEAK		SPREAD Depth (Å) σ_{peak}-50%σ_{peak}	FIGURE(S)
	σ(1/Ω-cm)	Depth (Å)		
S$^+$ 1E12 10.45	4.3E-4	530	490	11
S$^+$ 1E13 10.45	5.3E-1	500	500	12,13
S$^+$ 2E13 127.27	1.2E0	400	560	14
S$^+$ 1E14 10.45	3.0E0	250	650	15
S$^+$ 1E14 127.27	2.3E0	860	540	16
S$^+$ 1E15 127.27	1.4E0	1510	560	17
Te$^+$ 1E12 12.35	7.0E-2	85	130	18,19
Te$^+$ 1E13 12.35	1.3E0	260	375	20
Te$^+$ 1E13 123.46	1.2E0	360	240	21
Te$^+$ 1E14 12.35	6.7E-1	500	250	22
Te$^+$ 1E14 123.46	8.2E-1	250	320	23
Te$^+$ 1E15 123.46	1.8E0	300	165	24
Ar$^+$ 1E12 16.46	6.3E-4	280	315	25
Ar$^+$ 1E13 164.61	5.0E-1	165	660	26,27
Ar$^+$ 1E14 164.61	8.4E-1	225	1225	28
Ar$^+$ 1E15 164.61	1.0E0	1450	415	29

$$Z_i = \frac{(4.4 \times 10^{22})\,(\sigma_i)}{(\sigma_{max})} \tag{8}$$

where

Z_i = damage at point "i" (# atoms/cc)

σ_i = conductivity at point "i" $((\Omega\text{-cm})^{-1})$

Comparing Results with Theory

Figures 8, 9, and 10 show the resulting damage curves for S^+ and Ar^+ for doses of 1×10^{12}, 1×10^{13}, and 1×10^{14} and the damage curves for Te^+ for doses of 1×10^{12} and 1×10^{13}. On the graphs for S^+ and Te^+, the theoretical curves for these conditions are also plotted for comparison. For the case of Ar^+, the theoretical curves for S^+ can be used for an approximate comparison if desired. Higher doses are not considered because the theory fails to account for the damage saturation phenomena thus making any comparisons at higher doses invalid.

Conclusions

Several conclusions can be drawn from the material presented in this thesis. First, the differential electrical conductivity profile, as presented in this paper is a viable means of predicting damage distribution in ion-implanted GaAs. Figures 8, 9, and 10 show better than order-of-magnitude agreement between theory and experiment on all profiles except where $\emptyset$ equaled 1×10^{12} for S^+ and Ar^+. It has already been stated that theory and experiment will not agree in the higher dose ranges due to the saturation phenomena. Perhaps there is some similar explanation for the low dose range as well.
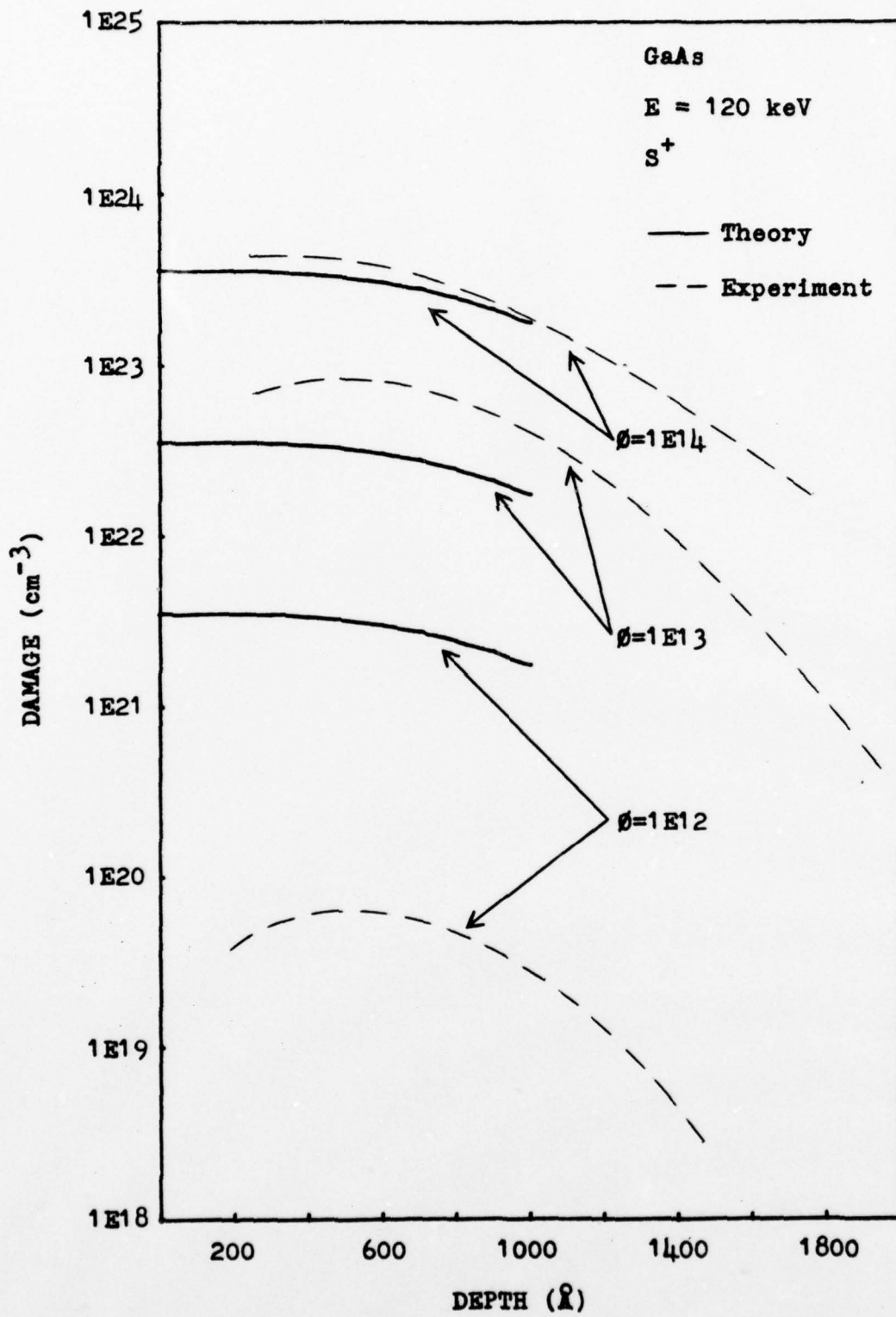
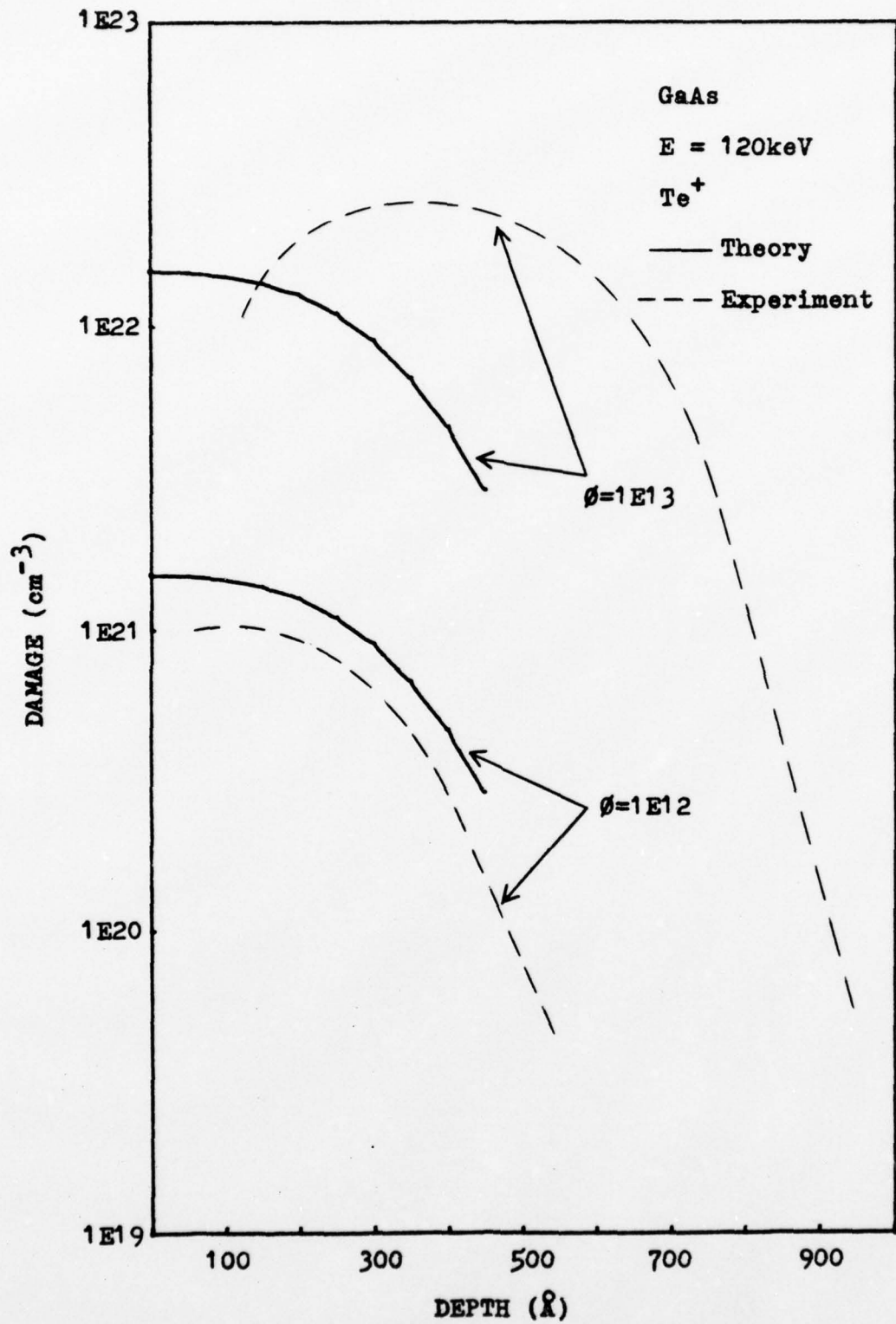Figure 8   Damage Profiles for S⁺
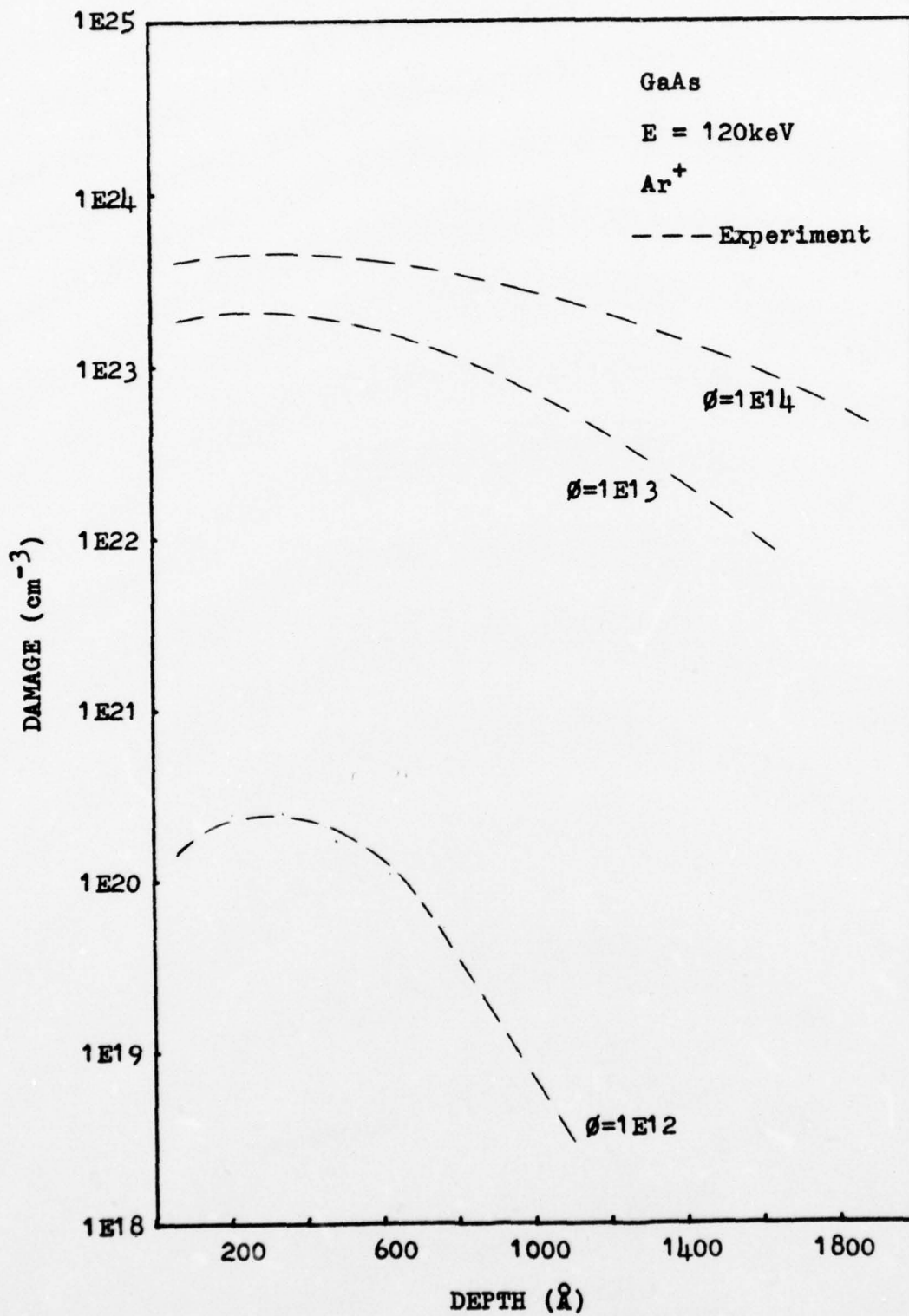
28

Figure 9   Damage Profiles for Te⁺

29

Figure 10   Damage Profiles for Ar+

Upon observing the conductivity profile curves in Appendix B for the higher dose rates, it can be concluded that above $\emptyset_{crit}$ the damage at the surface decreases due to the tendency for the excess energy to partially anneal the samples. The peak damage associated with $\emptyset_{crit}$ is still found, however, except that it is shifted deeper into the sample.

It can also be concluded that, as theory predicts, the damage tail does behave as an exponential decay. This is evidenced by the characteristic straight line plot of all the conductivity profile tails in Appendix B.

The fact that damage densities and not carrier concentrations are being measured can be concluded from the fact that Ar^+, a neutral dopant, produces curves similar to those for S^+ and Te^+ which are active dopants.

As table III shows, the flux at which these samples were implanted did not appear to have any significant influence on the damage distributions obtained. Samples of S^+ at 1×10^{14} and Te^+ at 1×10^{13} and 1×10^{14} were prepared using two different flux rates in order to evaluate this phenomena.

A final conclusion from this research program is that had there been more time to profile a larger number of samples from each of the sixteen catagories shown in Table II, the resulting curves would have reflected more accurately the nature of the damage density of ion-implanted GaAs. It is significant that even with so few samples, the results are within an order-of-magnitude of theoretical predictions.

VI   Suggestions and Recommendations

In the further development of the differential elec-
trical conductivity profile as a means of measuring damage,
there are several suggestions which seem appropriate based
upon the experience gained from this thesis. First, an
average profile required one full day to complete. This
lengthy time period necessarily reduced the number of
samples which could be measured. The technique presented
in this paper required many manual tasks which had to be
repeated many times. Also, a long waiting period between
each etch was required to obtain a stable reading. These
factors all contributed to the length of time required
to obtain one profile. It is suggested that an automated
system be developed in which a sample could be mounted
and then measured without the need for human interaction.
A small micro-processor could be tied into the system
which would analyze the incoming voltage and project its
final stable reading thus eliminating any need to wait
between etches. Taking this idea one step further, per-
haps this system could measure the sheet conductivity con-
tinuously (instead of in steps) as the surface is etched
by an acid bath. Using the micro-processor to compute the
derivitive of the sheet conductivity, the output of such a
system could be the conductivity profile itself.

The results of this thesis clearly show that the
damage-range theory does not consider the saturation or

self-annealing phenomenon at high doses and perhaps some other effects at low doses. It is suggested that the theory be refined to account for these observed deviations.

Finally, it is suggested that, using the DECP technique as a measure of damage, certain controllable parameters of the ion-implantation process can be changed and the resulting changes in damage recorded. These parameters might include capping, annealing, implanting at elevated temperatures, etc.. From these measurements a great deal can be learned about how to reduce and perhaps eliminate lattice damage in ion-implanted GaAs devices.

Bibliography

1. AFAL monthly status report. <u>Implantation Damage Studies by Conductivity Profiling</u>.

2. AFAL-TR-76-218. <u>Ion Implantation In Compound Semiconductors</u>. Washington: U.S. Government Printing Office, January 1977.

3. Gibbons, James F. "Ion Implantation in Semiconductors - Part I: Range Distribution Theory and Experiments," <u>Proceedings of the IEEE</u>, <u>56</u>: 295-319 (March 1968)

4. Anderson, Wayne J., Capt. <u>Electroreflectance Measurements of Radiation Damage in GaAs Caused by Ion-Implantation</u>. Paper prepared within the Air Force Avionics Laboratory/KHR. (Undated)

5. Gibbons, James F. "Ion Implantation in Semiconductors - Part II: Damage Production and Annealing," <u>Proceedings of the IEEE</u>, <u>60</u>: 1062-1096 (September 1972)

6. Shin, Bok K. Research Engineer, Systems Research Laboratories (personal interview). Wright-Patterson AFB, Ohio, August 31, 1978.

7. Mott, N. F. <u>Electronic Processes in Non-Crystalline Materials</u>. Glasgow: Oxford University Press, 1971.

8. AFAL monthly status report. <u>Conductivity Profile of Ion-Implanted GaAs</u>.

9. Gibbons, James F. <u>Projected Range Statistics in Semiconductors and Related Materials</u>, (2nd Edition). Stroudsburg, Pennsylvania: Dowden, Hutchinson and Ross, Inc., 1975.

Appendix A   Numerical Calculations for Critical Dose

$\emptyset_{crit}$ for GaAs is calculated from the following equation:

$$\emptyset_{crit} = N/((E_o)_n/E_d) \qquad (1)$$

where

N = Total number of atoms per unit volume of GaAs.
$(E_o)_n$ = Initial energy of incoming ion dissipated by nuclear collisions.
E_d = Energy required to displace a lattice atom.

For GaAs, $N \approx 4.4 \times 10^{22}$ atoms/cm^3 and $E_d \approx 18 \times 10^{-4}$ keV. Depending on the ion being implanted, the value of $(E_o)_n$ was determined from the charts in <u>Projected Range Statistics in Semiconductors and Related Materials</u> (2nd Edition). (Ref 9) These values are:

TABLE IV

Values of $(E_o)_n$ from Projected Range Tables

ION	$(E_o)_n$ (keV/cm)
S$^+$	$.4790 \times 10^6$
Te$^+$	$.3266 \times 10^7$
Ar$^+$	$.7078 \times 10^6$

The above numbers used in equation 1 give:

$$\emptyset_{crit} (S^+) = \frac{(4.4\times10^{22})\ (18\times10^{-4})}{(.4790\times10^6)} = 1.653 \times 10^{14}\ \text{ions/cm}^2 \qquad (9)$$

$$\emptyset_{crit} (Te^+) = \frac{(4.4\times10^{22})\ (18\times10^{-4})}{(.3266\times10^7)} = 2.425 \times 10^{13}\ \text{ions/cm}^2 \qquad (10)$$

$$\emptyset_{crit} (Ar^+) = \frac{(4.4\times10^{22})\ (18\times10^{-4})}{(.7078\times10^6)} = 1.119 \times 10^{14}\ \text{ions/cm}^2 \qquad (11)$$

Appendix B   Conductivity Profiles

The graphs contained in this Appendix represent the
total experimental effort put forth for this thesis. In
most cases, when two samples of the same type were pro-
filed, the data points they generated were placed on a
single graph. When the two profiles were significantly
different, they were plotted on separate graphs.

The curves were drawn using a french curve. In some
cases, estimates of true values different from the measured
points were made (shown by dashed lines). These were done
when it was felt that the experimental technique caused
false values of conductivity to be measured. These false
readings occurred in two places. First, near the surface,
the measured values tended to be unreliable due to surface
effects such as oxide layers and dirt. Second, through the
course of measuring some samples it is believed that the
contacts were partially broken causing the measured values
of conductivity to shift. Uncorrected, this effect would
tend to shift the latter portion of the curves over and up
creating the impression of a wider distribution than actually
existed. Figure 18 is a good example of this phenomenon.
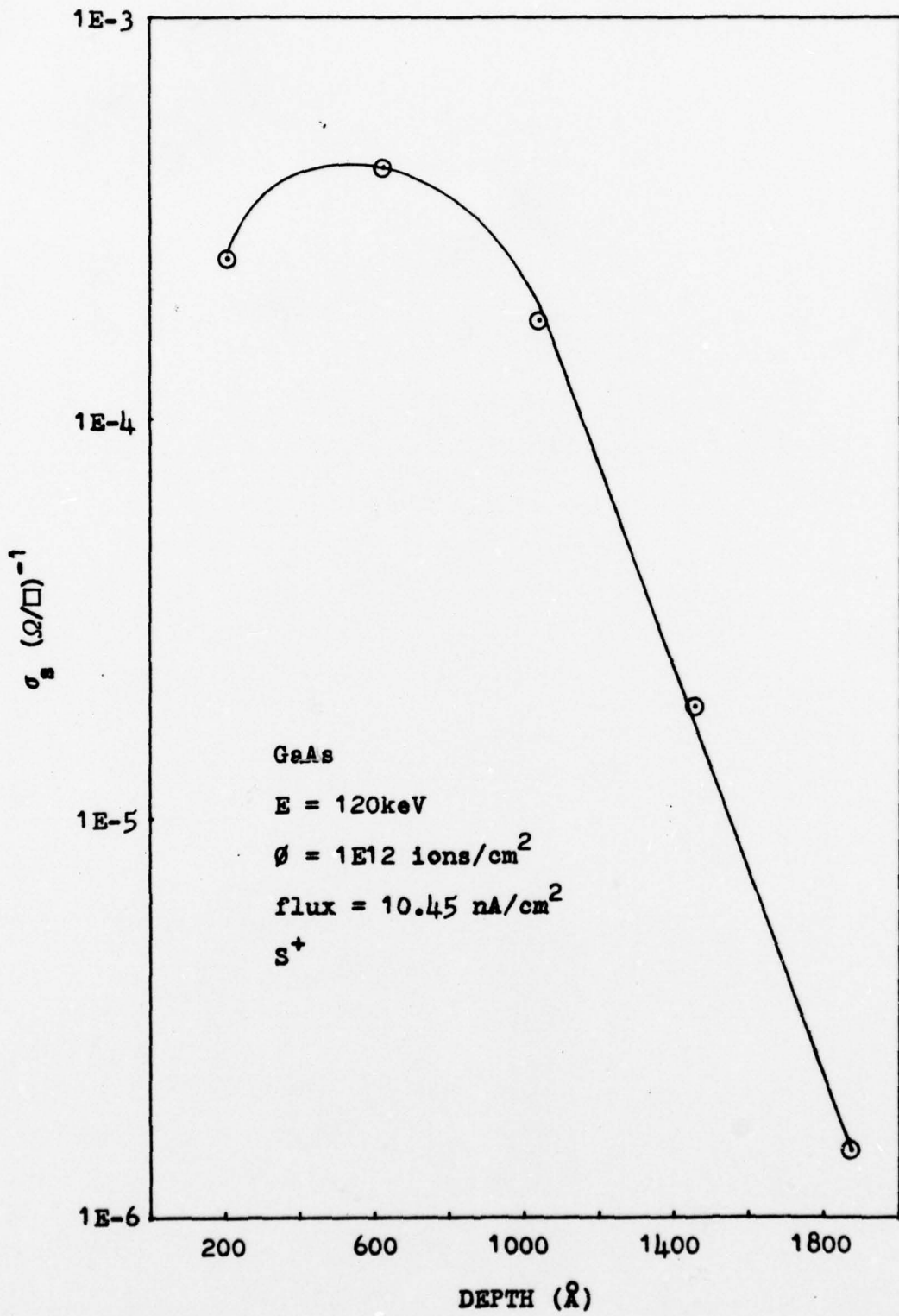
Figure 11   Conductivity Profile, S$^+$

37
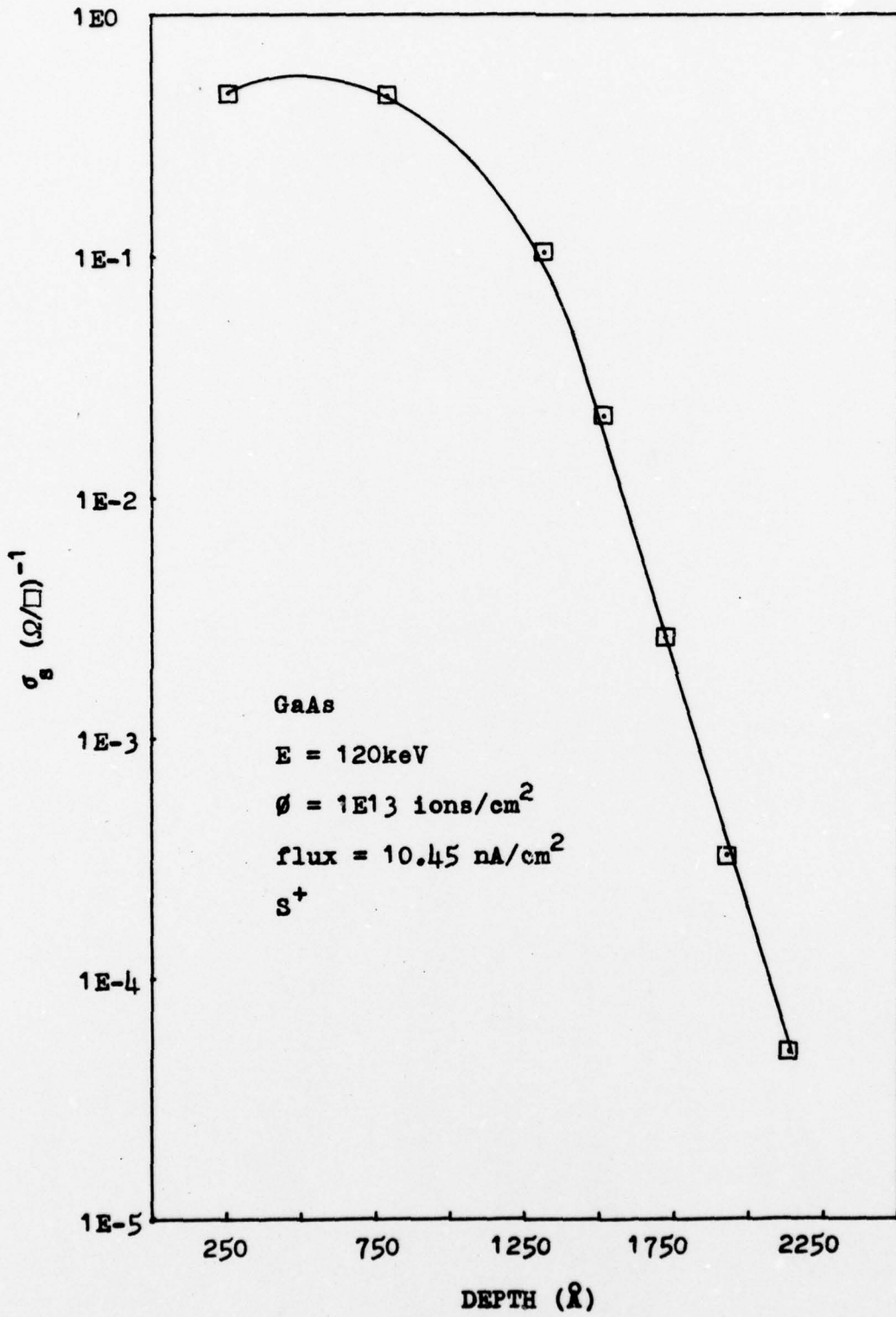
Figure 12   Conductivity Profile, S⁺

38
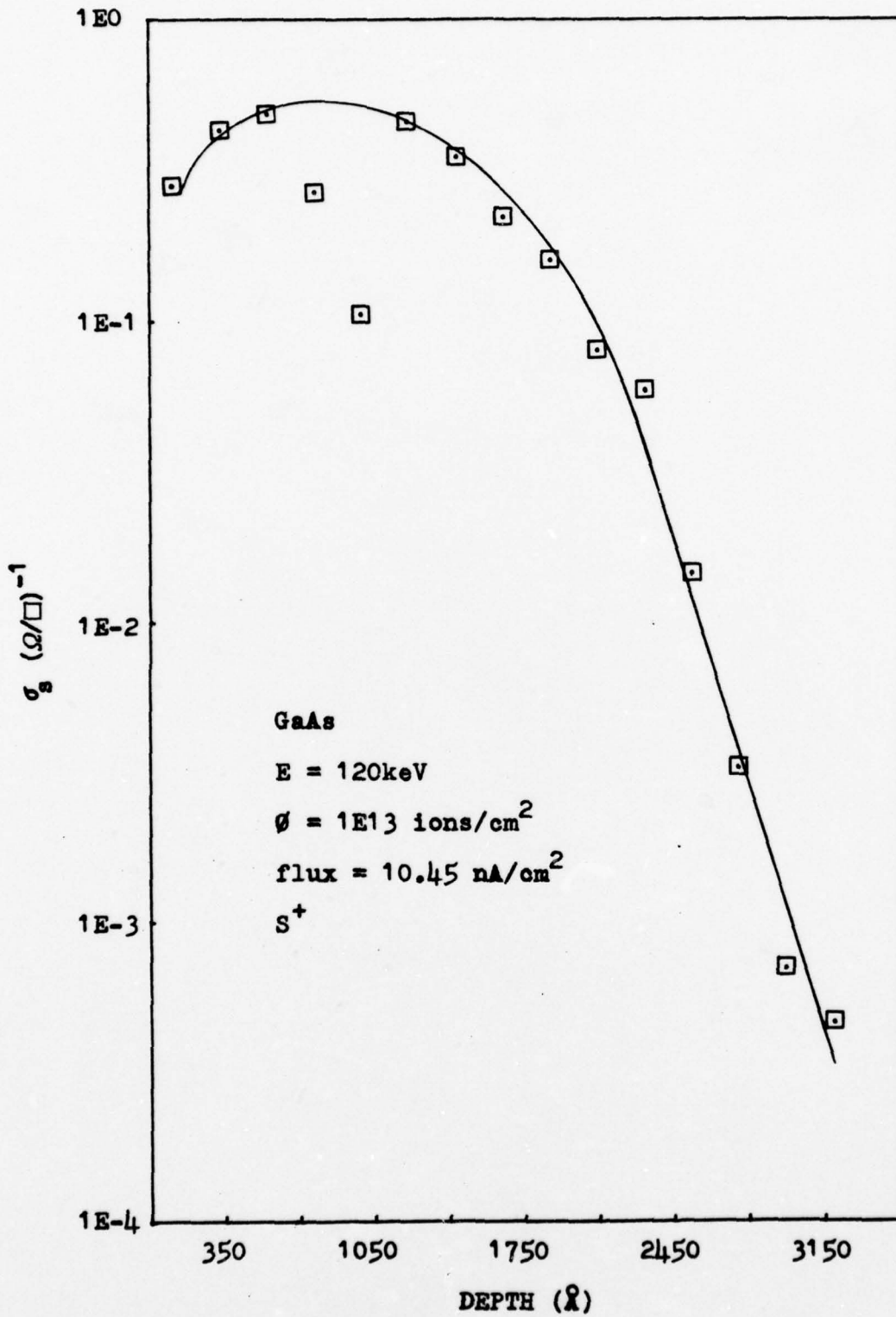
Figure 13   Conductivity Profile, S⁺

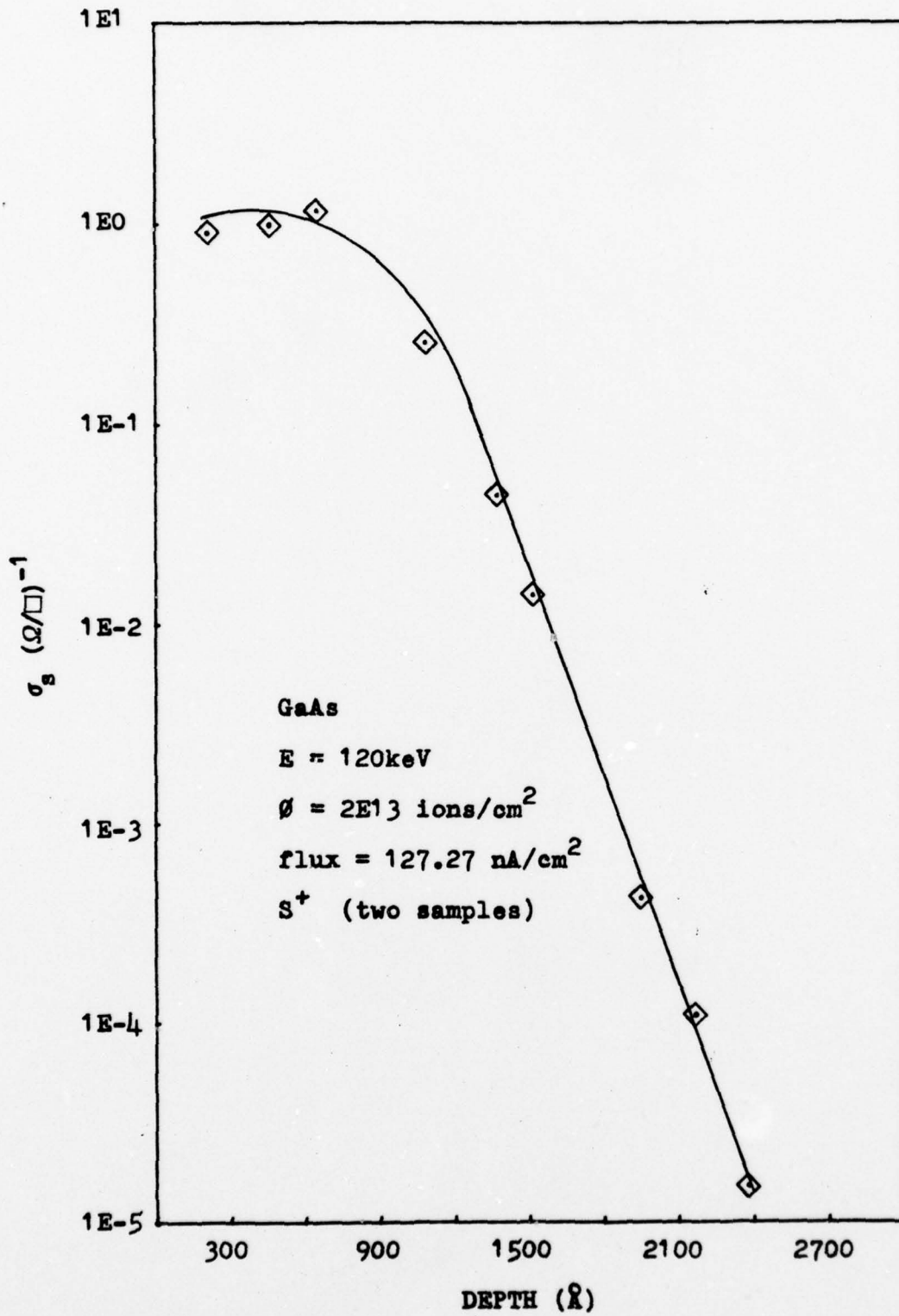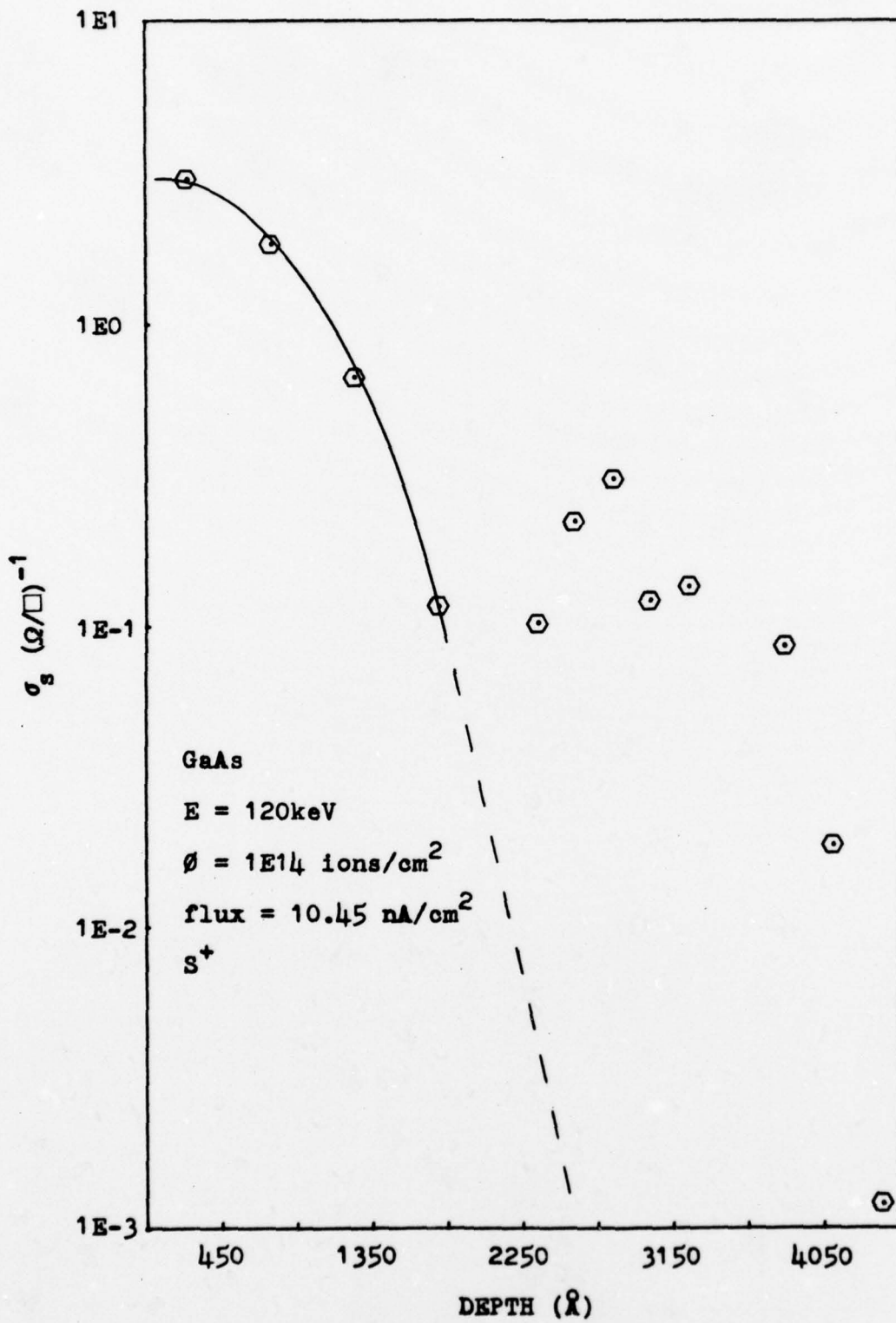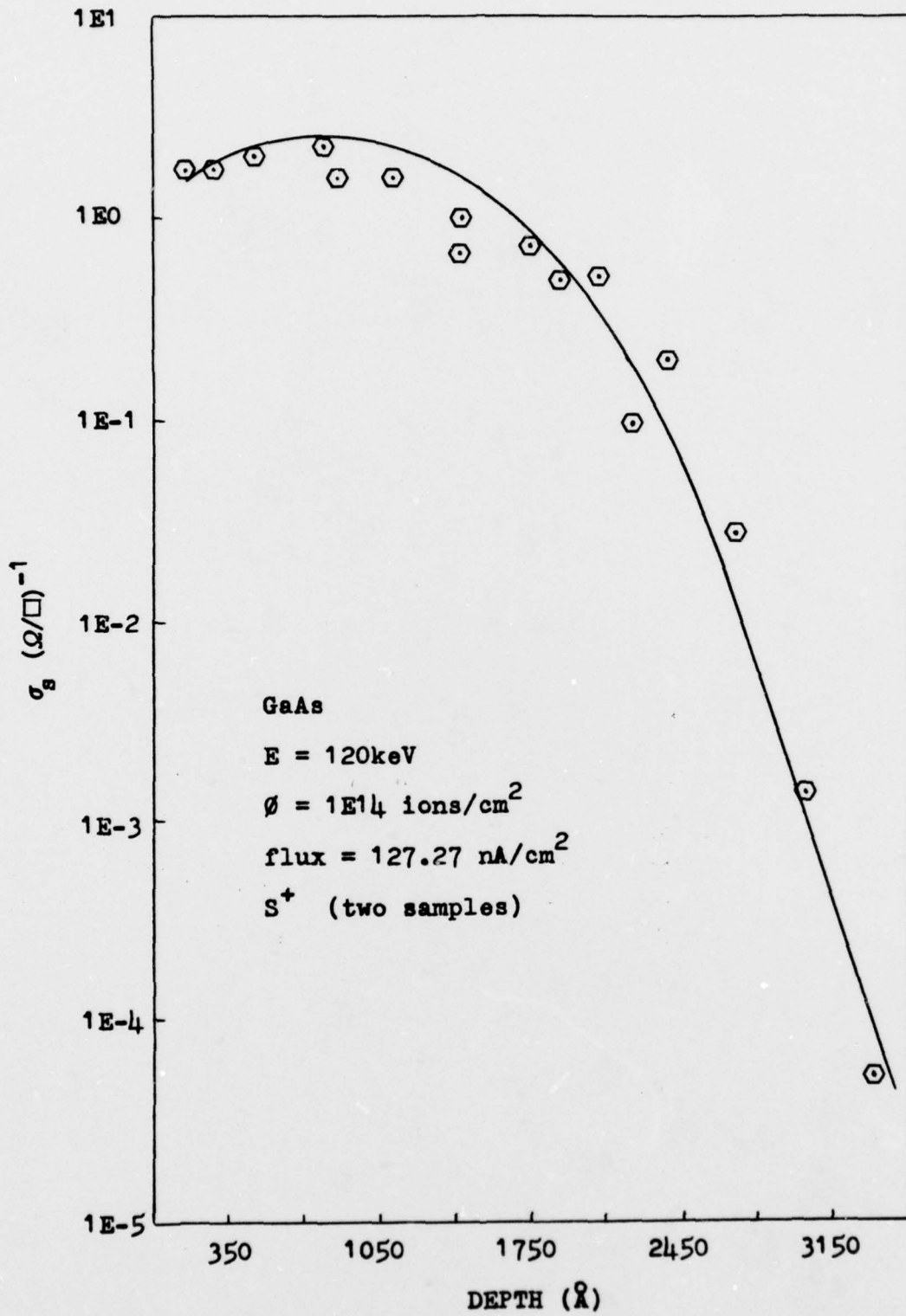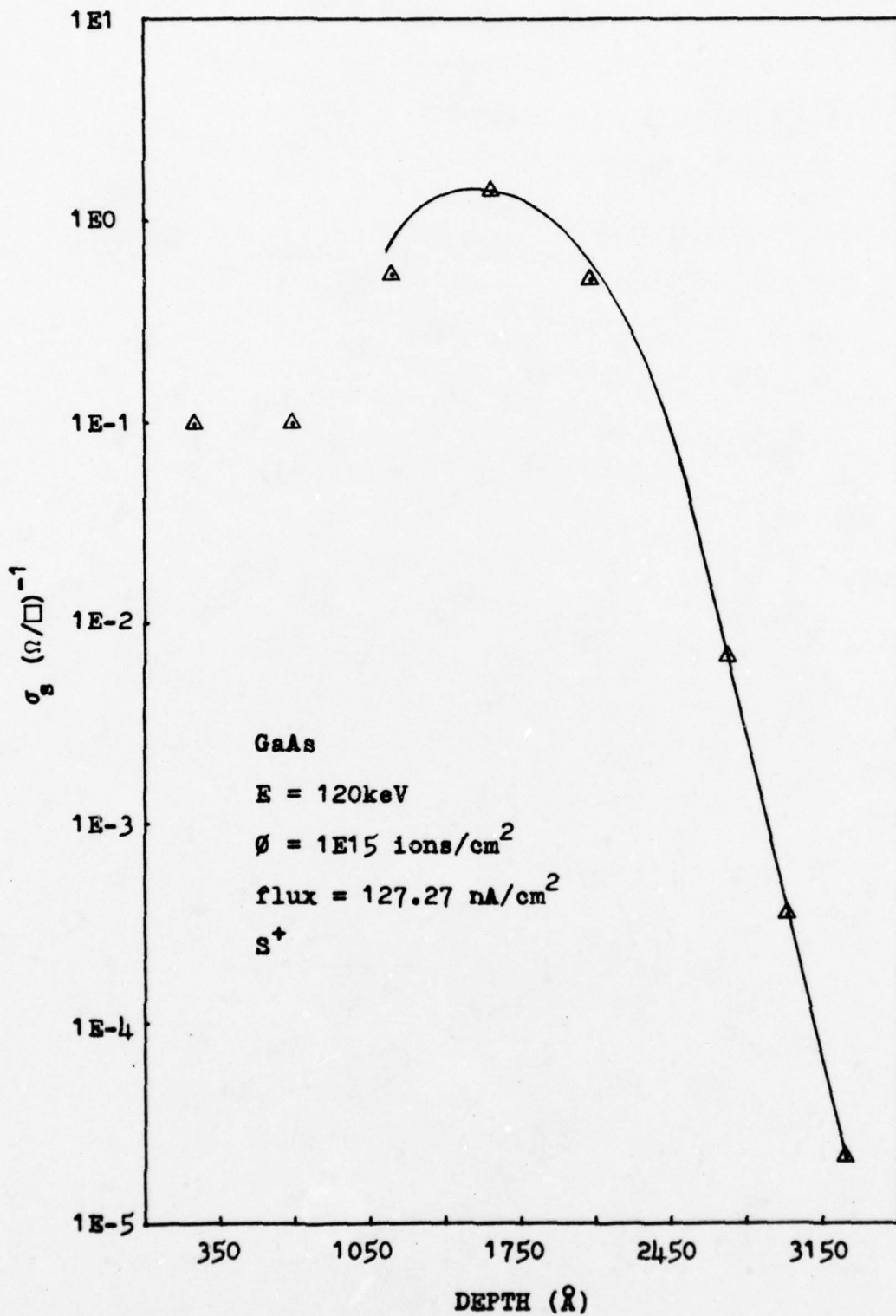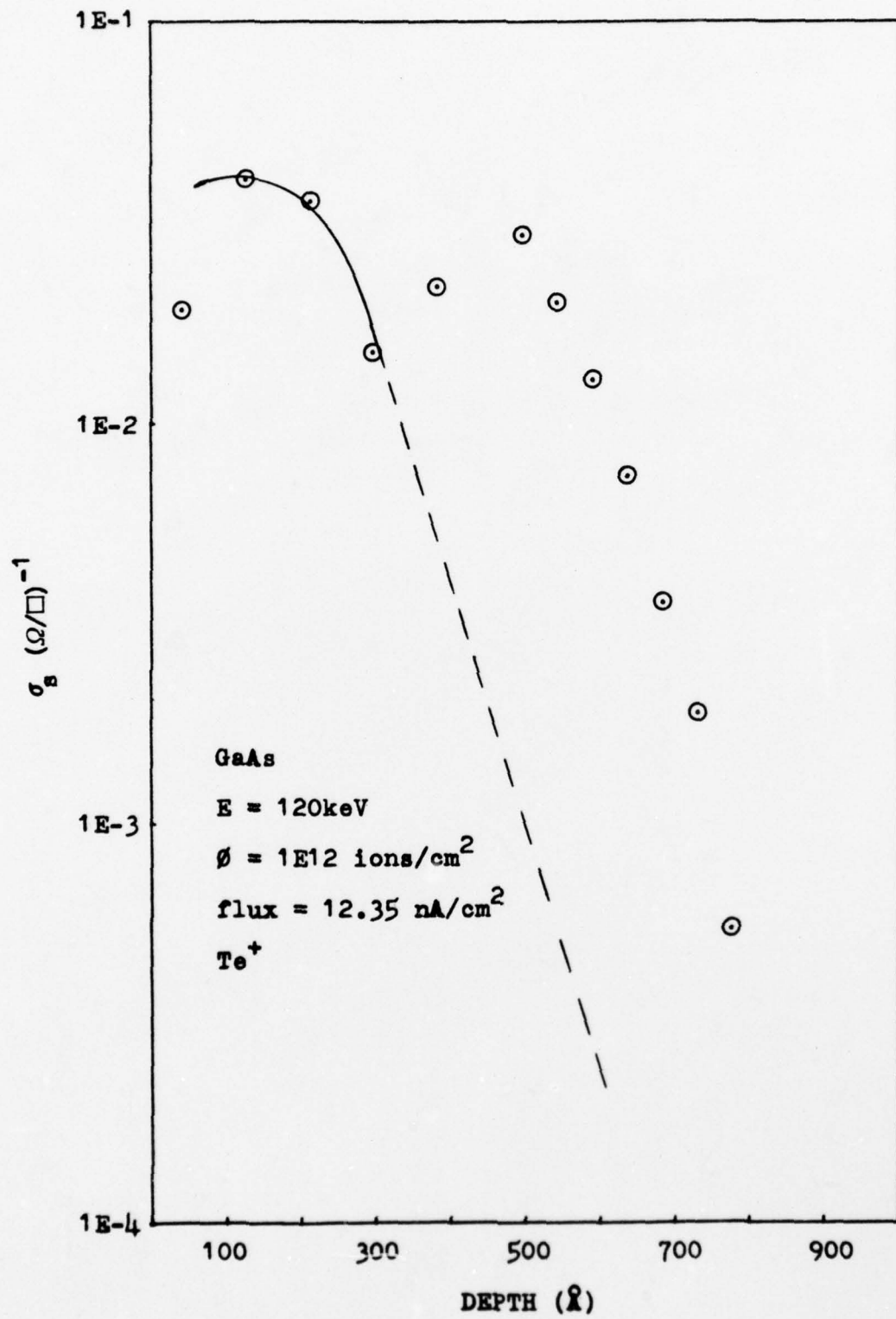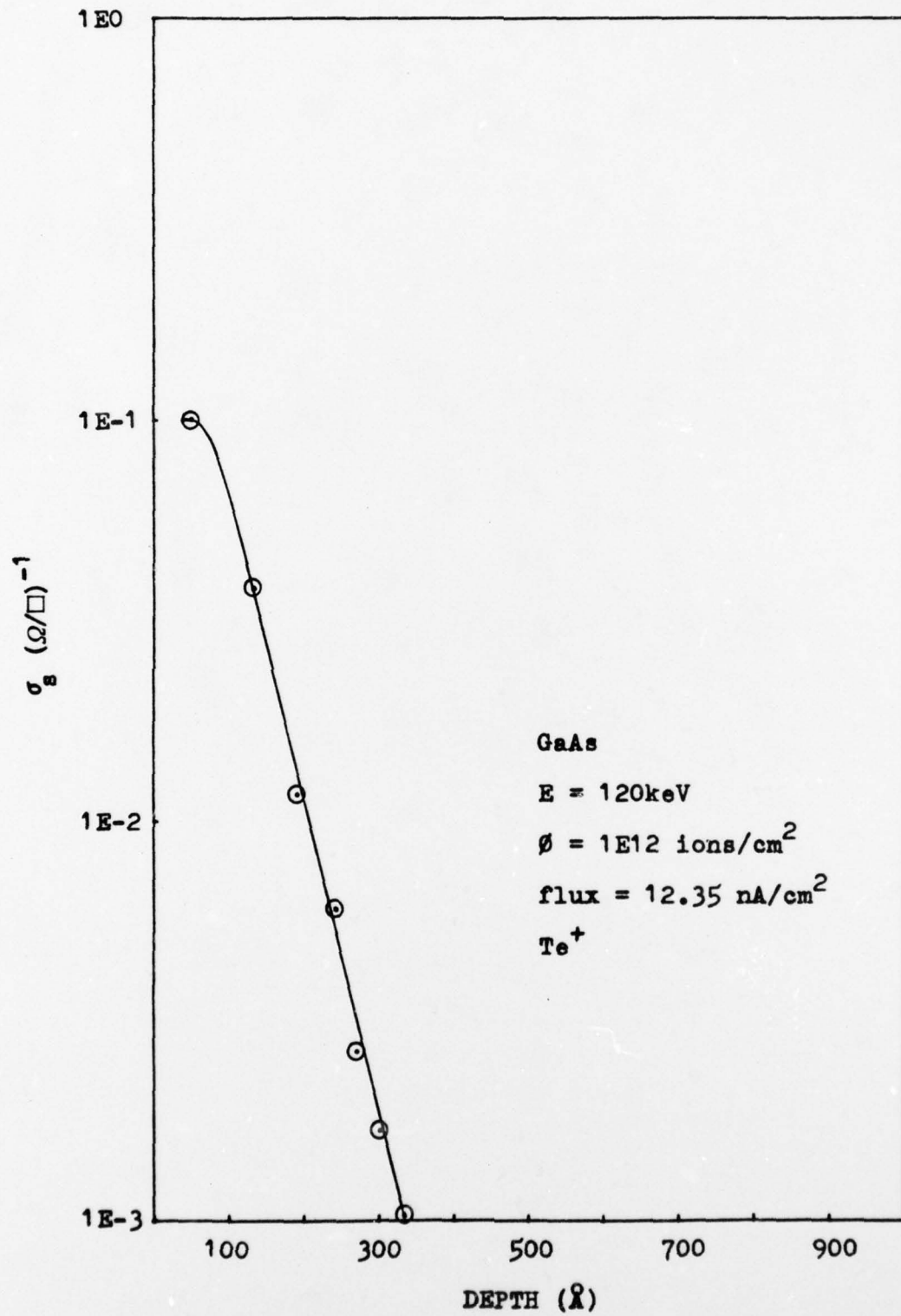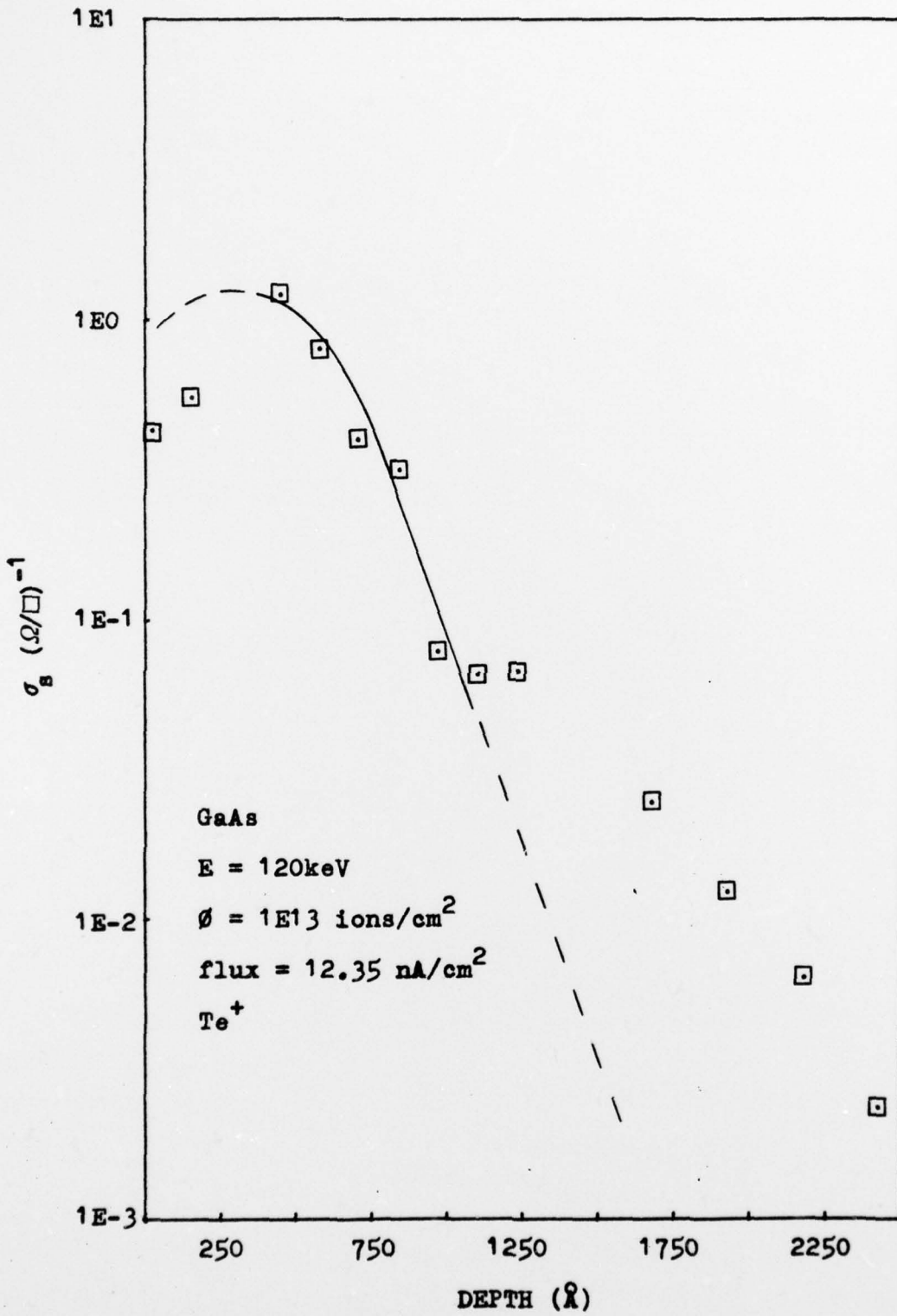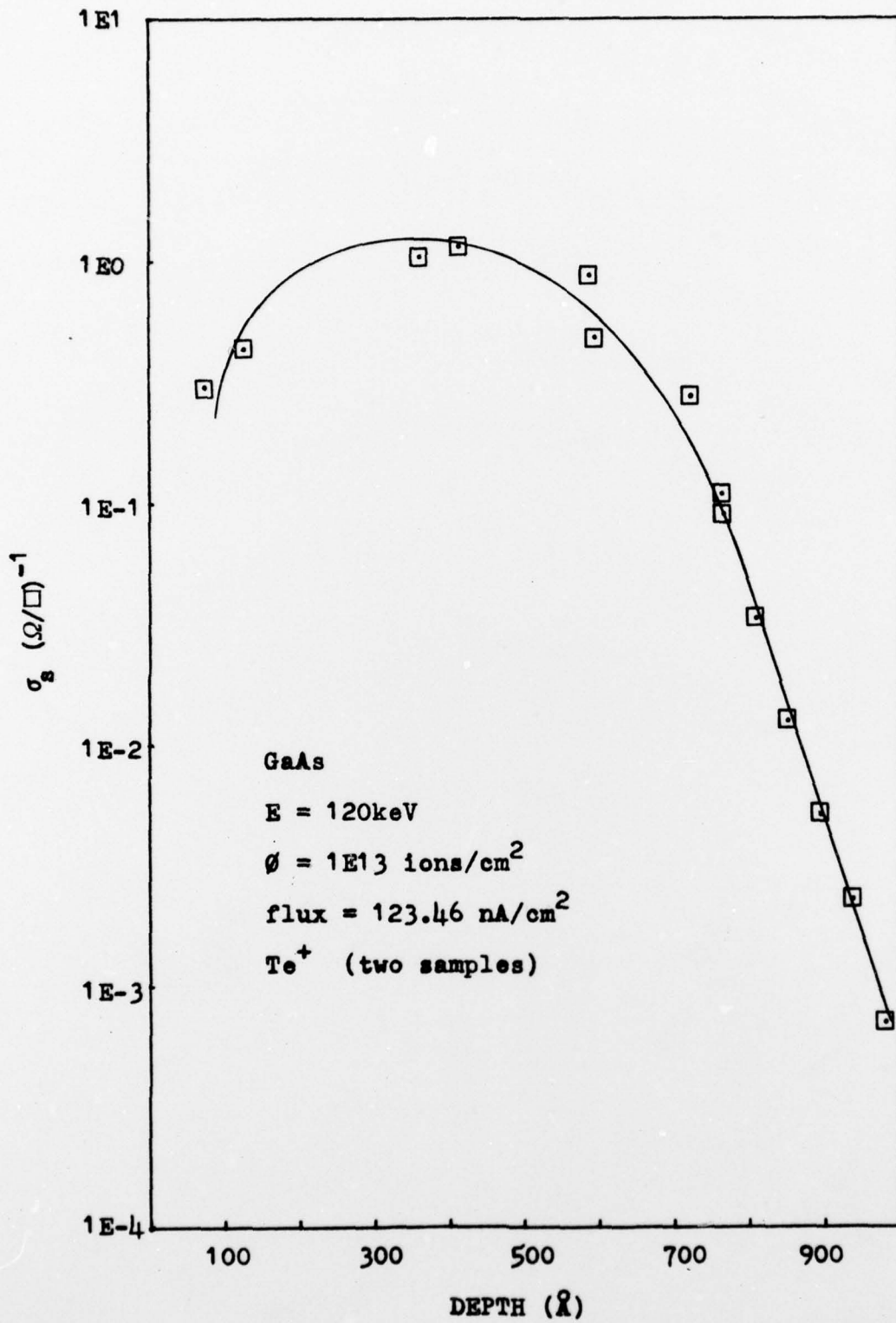Figure 14   Conductivity Profile, S⁺

Figure 15   Conductivity Profile, S+

Figure 16   Conductivity Profile, S⁺

42

Figure 17   Conductivity Profile, S$^+$

Figure 18   Conductivity Profile, Te⁺

44

Figure 19   Conductivity Profile, Te+

45

Figure 20   Conductivity Profile, Te$^+$

46

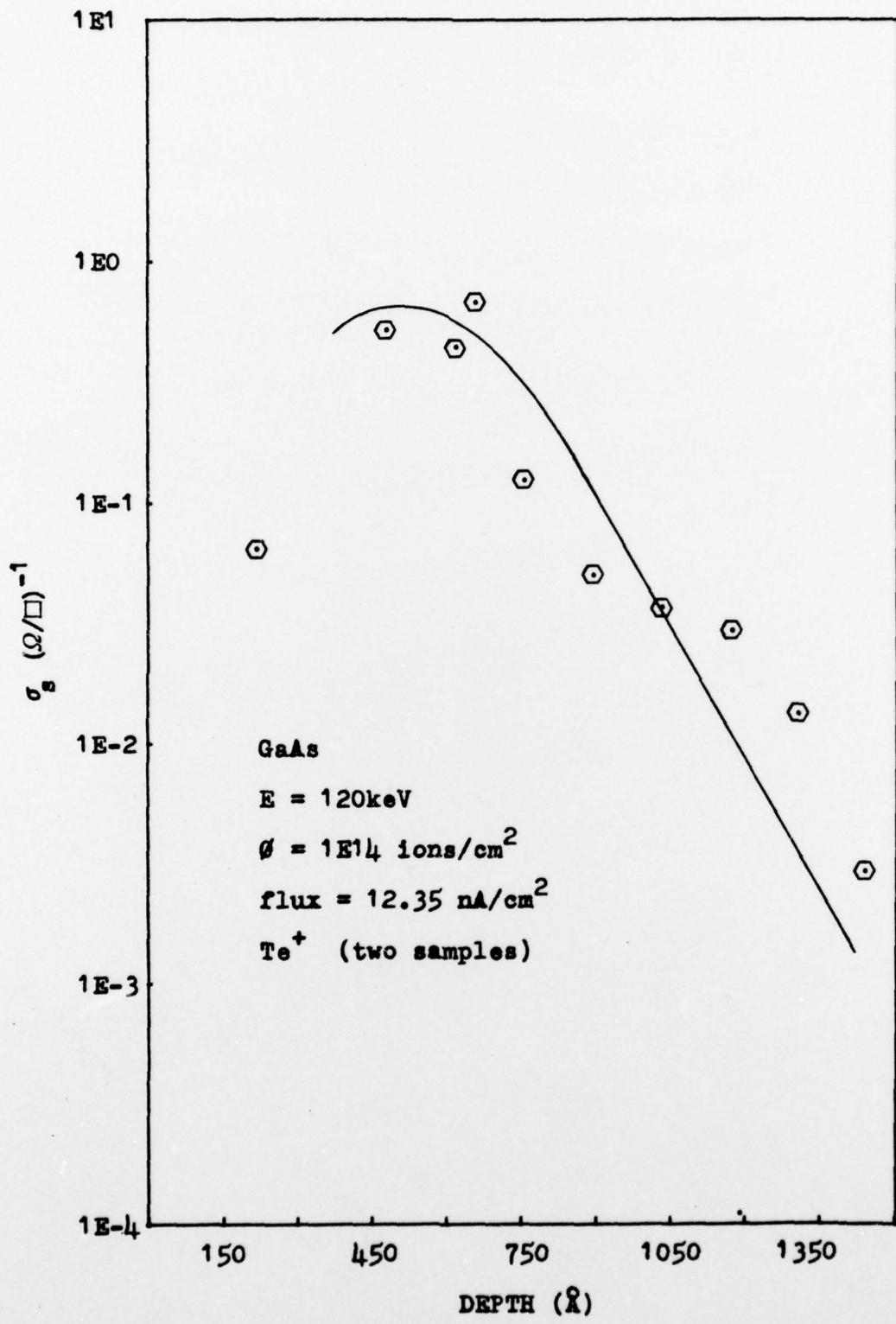Figure 21   Conductivity Profile, Te$^+$

47

Figure 22   Conductivity Profile, Te$^+$
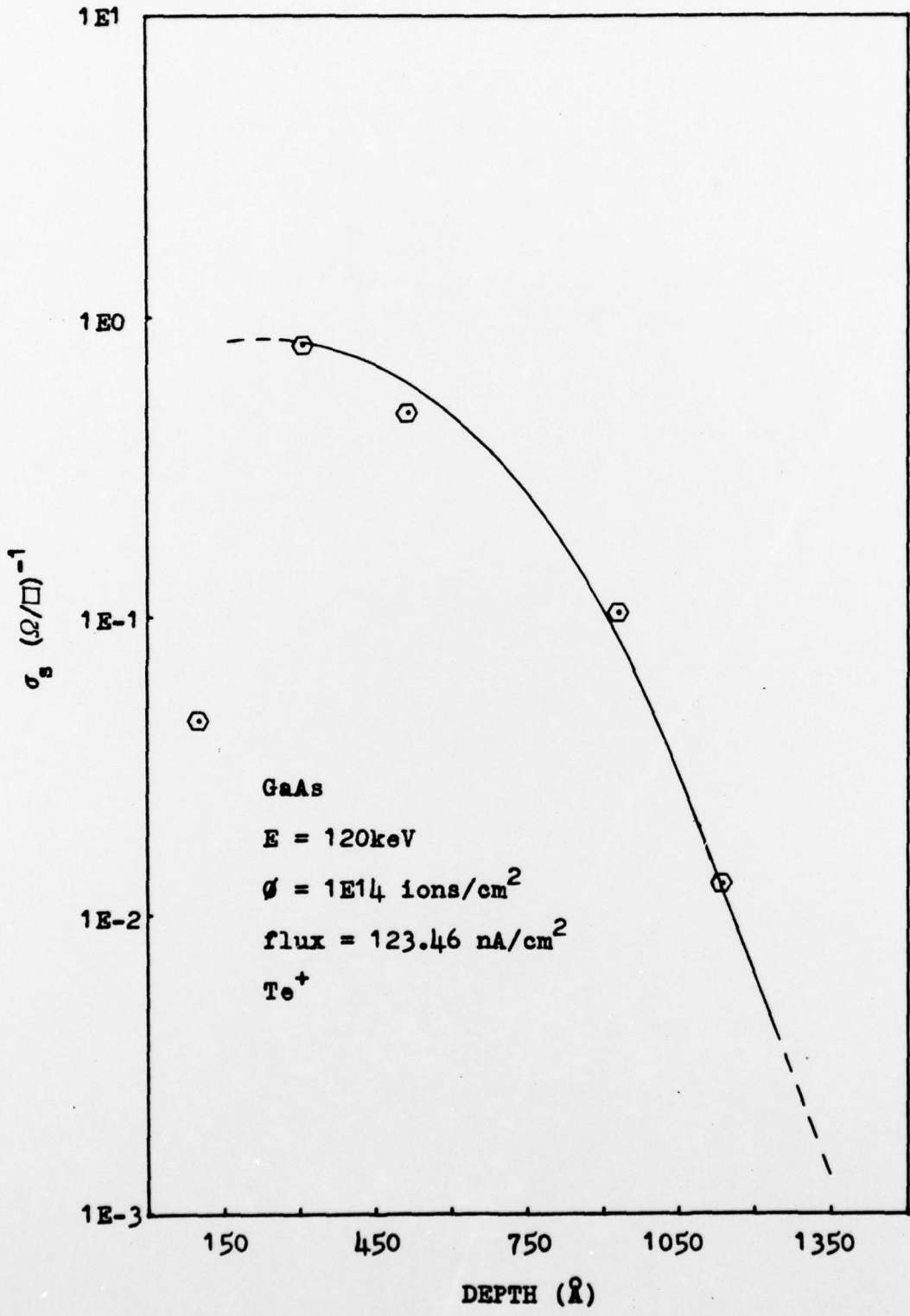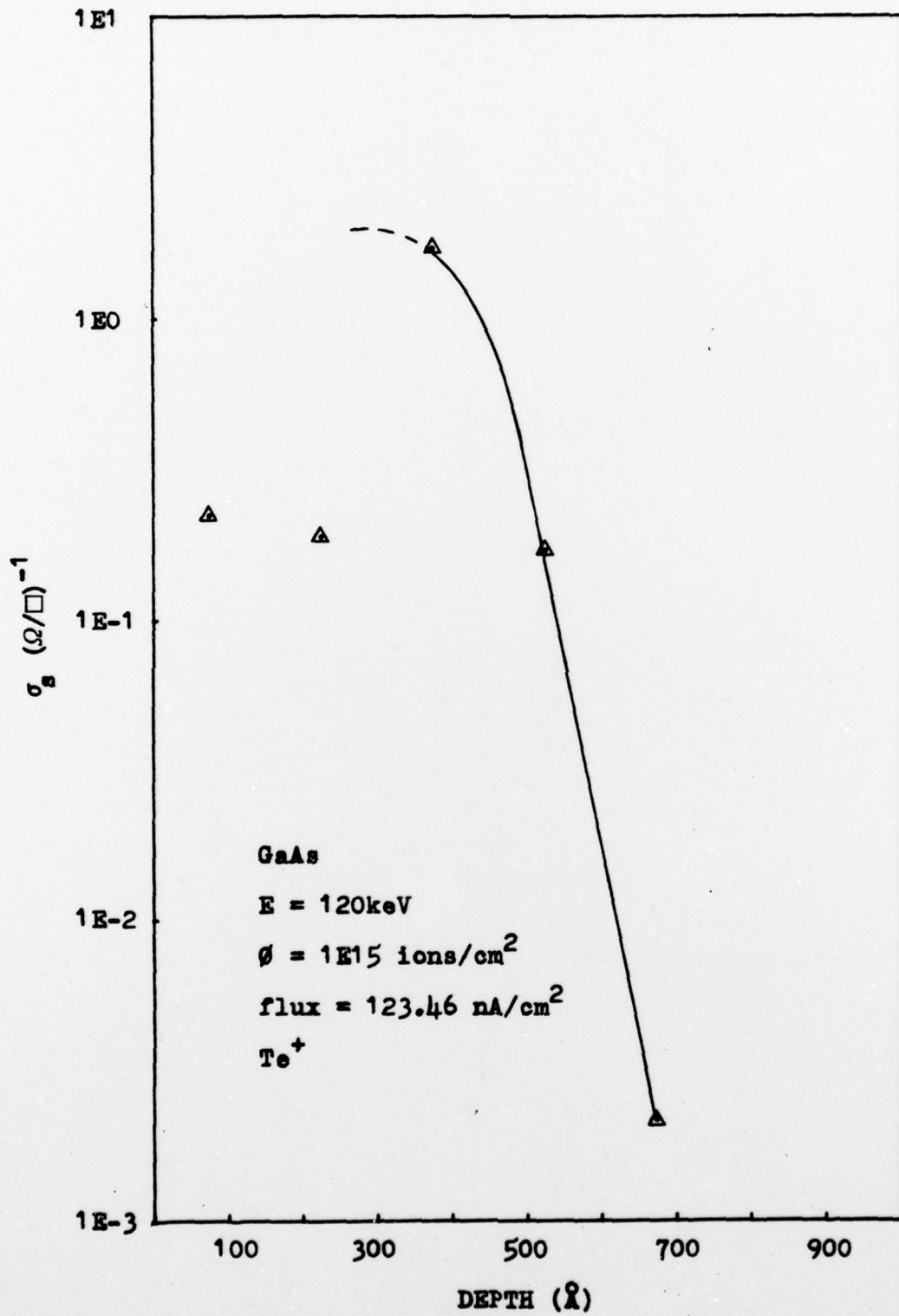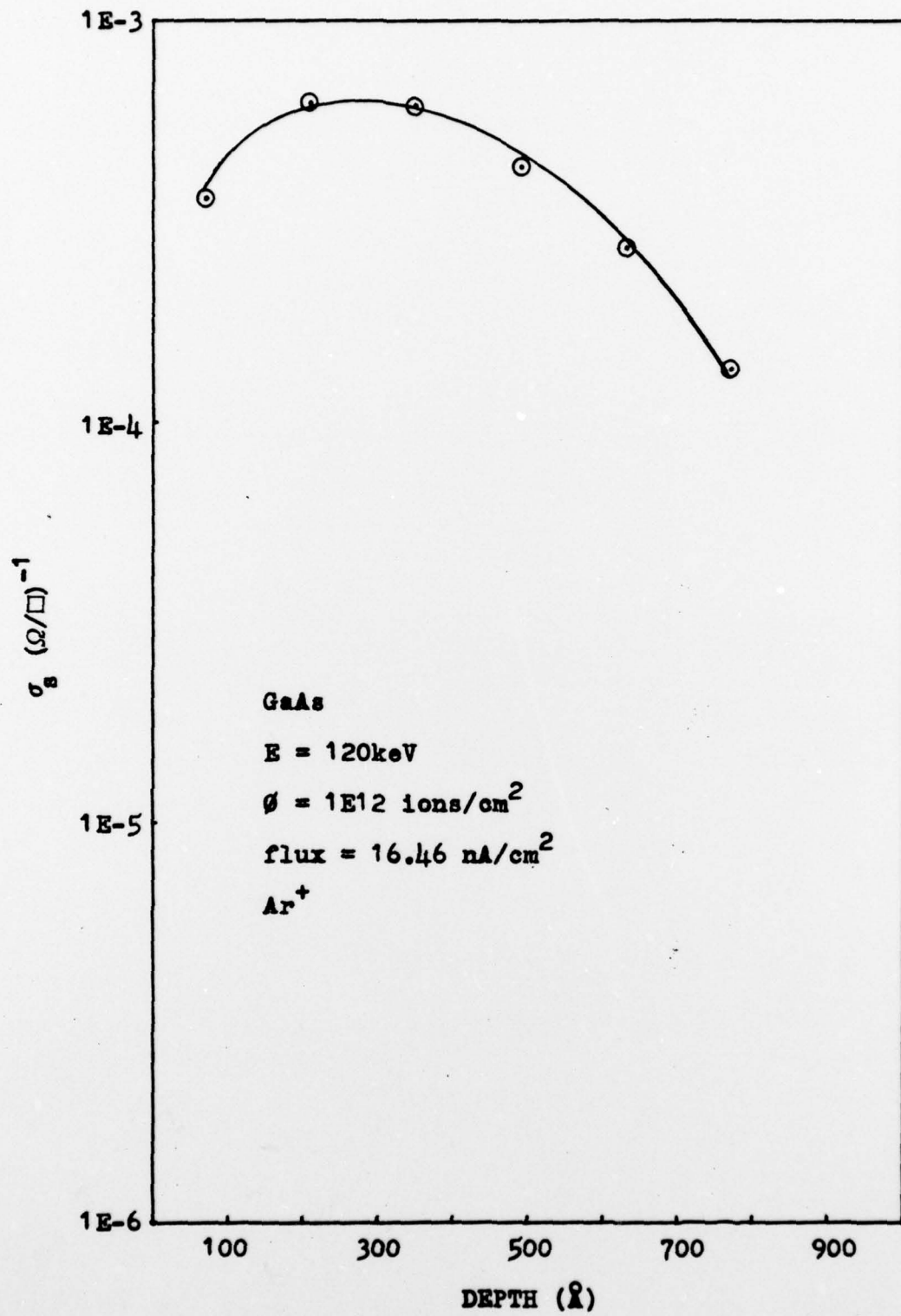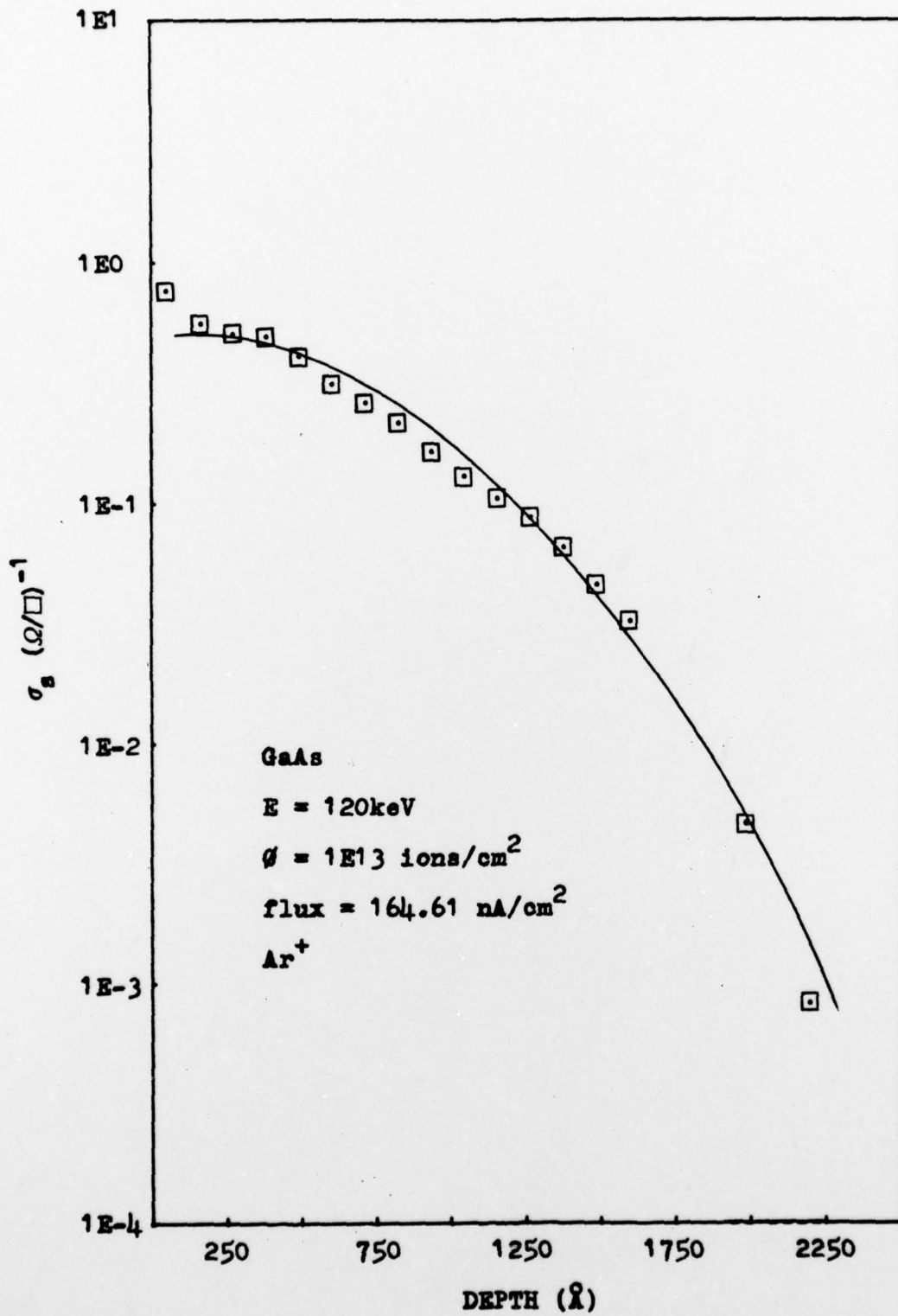
48

Figure 23   Conductivity Profile, Te$^+$

Figure 24   Conductivity Profile, Te$^+$

Figure 25   Conductivity Profile, Ar⁺

1E1

1E0

1E-1

$\sigma_s \ (\Omega/\square)^{-1}$

1E-2

GaAs

E = 120keV

∅ = 1E13 ions/cm^2

flux = 164.61 nA/cm^2

Ar$^+$

1E-3

1E-4

250   750   1250   1750   2250

DEPTH (Å)

Figure 26   Conductivity Profile, Ar$^+$

52
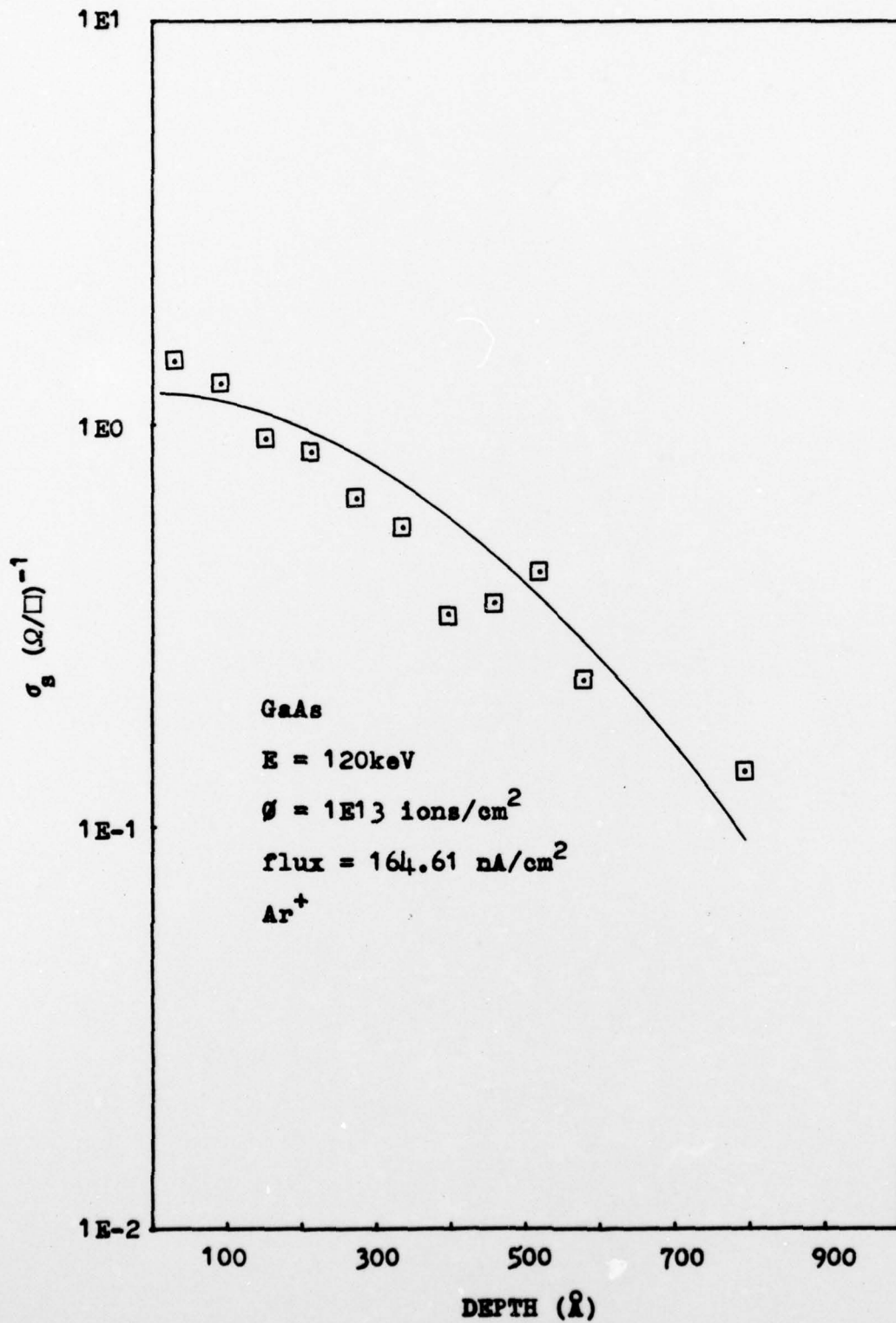
Figure 27   Conductivity Profile, Ar$^+$

The figure shows a plot with vertical axis labeled σ_s $(\Omega/\square)^{-1}$ with values from 1E-2 to 1E1, and horizontal axis labeled DEPTH (Å) with values from 100 to 900.

GaAs

E = 120keV

$\emptyset$ = 1E13 ions/cm^2
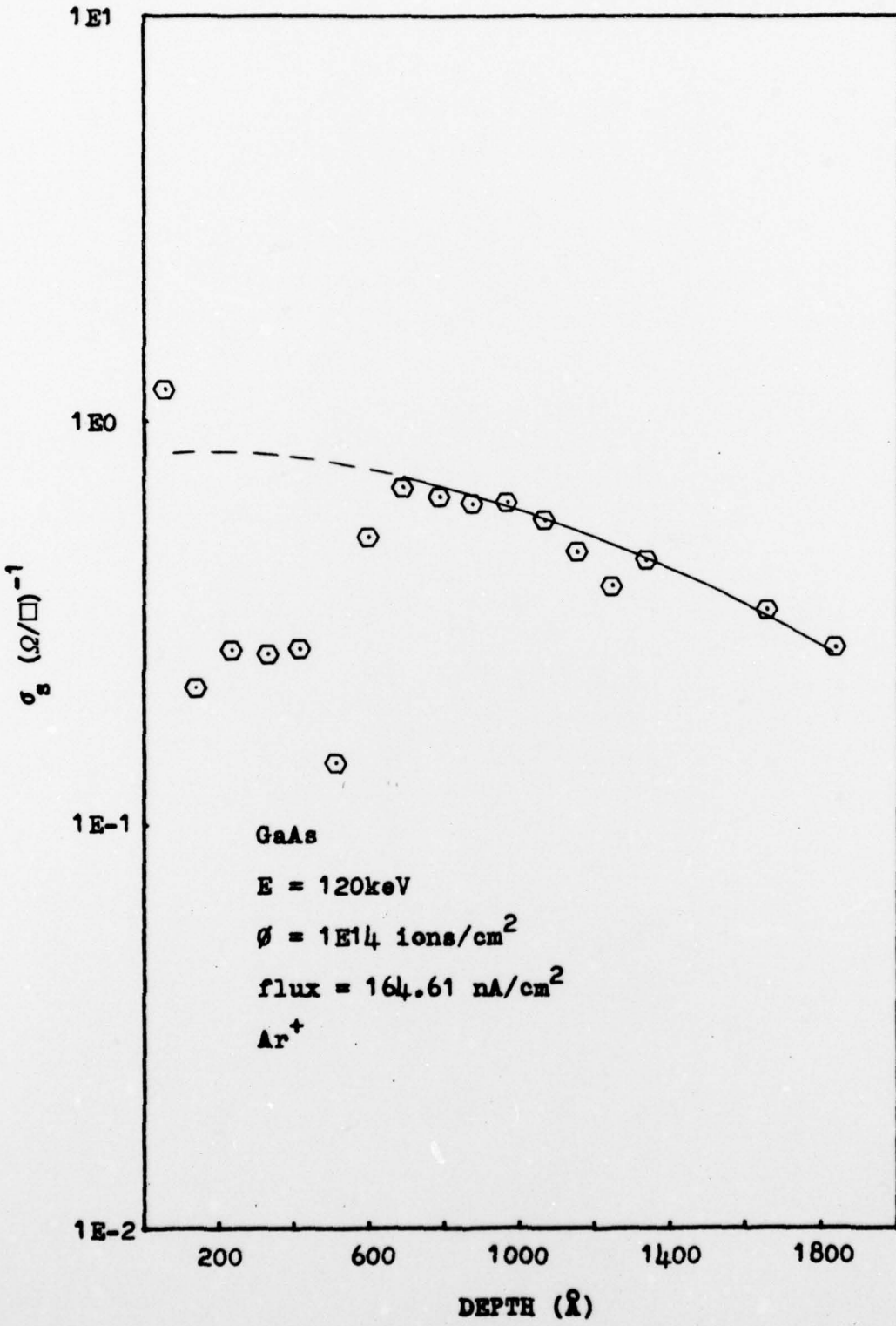
flux = 164.61 nA/cm^2

Ar$^+$

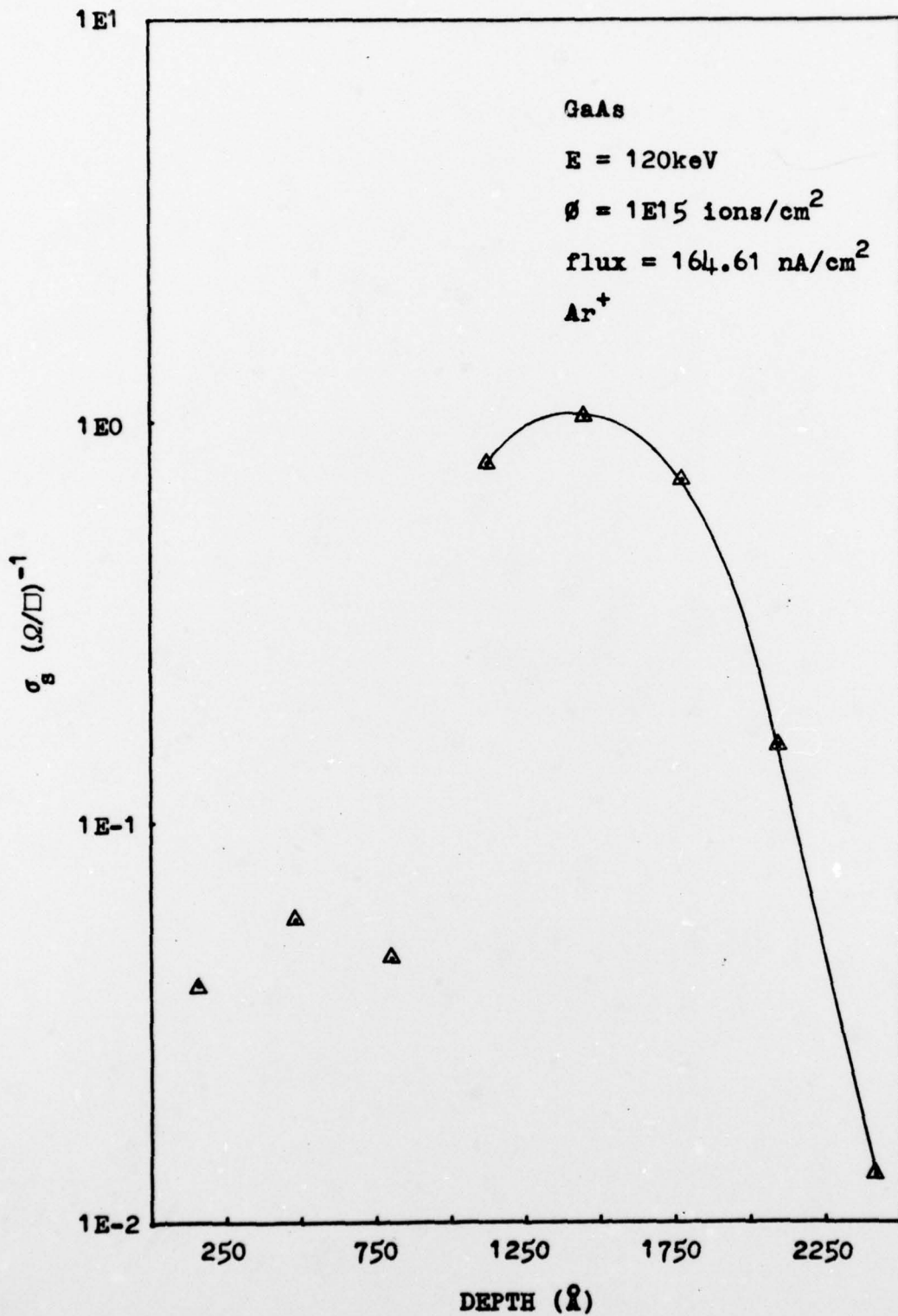Figure 28   Conductivity Profile, Ar+

54

Figure 29   Conductivity Profile, Ar+

VITA

Russell McAllister Solt, III was born on 18 February 1952 in Perth Amboy, New Jersey. Most of his childhood years, however, were spent in California. He graduated from high school in Fountain Valley, California in 1970 and attended the United States Air Force Academy from which he received the degree of Bachelor of Science in Electrical Engineering and his commission in the USAF in June of 1974. He served in the position of NAF electronic engineer for Hq. Air Weather Service at Scott AFB, Illinois prior to entering the School of Engineering, Air Force Institute of Technology, in June 1977.

Permanent address: 124 Mosscreek Rd.
El Toro, California 92630

REPORT DOCUMENTATION PAGE		READ INSTRUCTIONS BEFORE COMPLETING FORM
1. REPORT NUMBER AFIT/GE/EE/78D-43	2. GOVT ACCESSION NO.	3. RECIPIENT'S CATALOG NUMBER
4. TITLE (and Subtitle) DAMAGE STUDIES OF ION-IMPLANTED GaAs USING CONDUCTIVITY PROFILES		5. TYPE OF REPORT & PERIOD COVERED MS Thesis
		6. PERFORMING ORG. REPORT NUMBER
7. AUTHOR(s) Russell M. Solt Capt.		8. CONTRACT OR GRANT NUMBER(s)
9. PERFORMING ORGANIZATION NAME AND ADDRESS Air Force Institute of Technology (AFIT-EN) Wright-Patterson AFB, Ohio 45433		10. PROGRAM ELEMENT, PROJECT, TASK AREA & WORK UNIT NUMBERS
11. CONTROLLING OFFICE NAME AND ADDRESS Air Force Avionics Laboratory Electronic Research Branch (AFAL/DHR) Wright-Patterson AFB, Ohio 45433		12. REPORT DATE December, 1978
		13. NUMBER OF PAGES 65
14. MONITORING AGENCY NAME & ADDRESS(if different from Controlling Office)		15. SECURITY CLASS. (of this report) Unclassified
		15a. DECLASSIFICATION/DOWNGRADING SCHEDULE

16. DISTRIBUTION STATEMENT (of this Report)

Approved for public release; distribution unlimited.

17. DISTRIBUTION STATEMENT (of the abstract entered in Block 20, if different from Report)

18. SUPPLEMENTARY NOTES

Approved for public release; IAW AFR 190-17

1-23-79   Joseph P. Hipps, Maj.
Director of Information

19. KEY WORDS (Continue on reverse side if necessary and identify by block number)

Differential Electrical Conductivity Profile
Damage Profile
Conductivity Profile
Ion Implantation
Galium Arsenide

20. ABSTRACT (Continue on reverse side if necessary and identify by block number)

The understanding of damage produced during ion-implantation
is an important first step towards predicting the semiconducting
behavior of GaAs samples. A new technique for measuring damage
has been developed by the Air Force Avionics Laboratory. This
method involves the measurement of a differential electrical
conductivity profile.

Samples of GaAs doped with S^+, Te^+ and Ar^+ ions were pre-
pared for the purpose of profiling them with this technique.

DD FORM 1473 1 JAN 73   EDITION OF 1 NOV 65 IS OBSOLETE

Prior to measurement, theoretical values of critical dose and theoretical damage profiles were calculated using damage-range theory.

Values of sheet conductivity were measured with an electrical measurement system. Twenty-three samples of varying dose, flux and implant type were used. Each sample was profiled by measuring sheet conductivity at successively deeper levels into the sample. A solution of H_2SO_4 : H_2O_2 : H_2O was used to etch the samples to arrive at these deeper levels. The thickness etched away was determined by the use of a Sloan Dektak Surface Profile Measuring System.

The values of sheet conductivity measured along with the thickness etched away were used to create bulk conductivity profiles for all of the samples. The normalized profiles are used to show damage versus depth. The measured values of critical dose and damage agree within an order of magnitude of those predicted by theory.